2/51

DETAILED REVIEW OF SELECTED ASPECTS OF TOTAL SYSTEM PERFORMANCE ASSESSMENT — 1995

Prepared for

Nuclear Regulatory Commission
Contract NRC-02-93-005

Edited by

Robert G. Baca
Mark S. Jarzemba

Center for Nuclear Waste Regulatory Analyses
San Antonio, Texas

February 1997

EXECUTIVE SUMMARY

As directed by the Nuclear Regulatory Commission (NRC), the Center for Nuclear Waste Regulatory Analyses (CNWRA) performed a detailed review of selected aspects of the U.S. Department of Energy (DOE) Total System Performance Assessment—1995 (TSPA-95) report. The review builds on the previous audit review of TSPA-95 that the NRC transmitted to the DOE in July 1996. The purpose of this review was to provide early feedback to the DOE regarding potential vulnerabilities of their TSPA methodology. This information is intended to aid the DOE in their on-going preparations for the TSPA-Viability Assessment.

Due to resource constraints, it was decided that this review should address a limited number of focus topics. Initially, the detailed review focused on six important topics: (i) container lifetime, (ii) percolation flux, (iii) fracture/matrix interactions (i.e., matrix diffusion effects), (iv) faulting scenario (not considered in TSPA-95), (v) volcanism scenario (not considered in TSPA-95), and (vi) TSPA abstractions (i.e., propagating the effects of container lifetimes, percolation flux, and matrix diffusion). Of the detailed analyses conducted for these focus topics, only three produced results of substantial difference from TSPA-95 and merit transmittal to the DOE at this time. Topics not discussed in this report are being addressed in ongoing technical studies; important findings from these studies will be communicated to DOE in future CNWRA reports and NRC/DOE technical studies. The three topics that are addressed in this report are container lifetime, fracture/matrix interactions, and volcanism scenario.

For each of the focus topics, the CNWRA reviewed the TSPA-95 with respect to the appropriateness of the technical approach (i.e., conceptual and mathematical models), consistency of models with interpretations of available data, adequacy of the treatment of uncertainties (i.e., parameter, conceptual model, and future system states), and use of conservative and bounding assumptions. The review approach was based on performing independent analyses using a combination of simplified and detailed TSPA models.

This detailed review of the DOE methodology and analyses in TSPA-95 produced the following major comments:

Container Lifetime

- The DOE container lifetime code, WAste Package DEGradation (WAPDEG), does not consider corrosion processes enhanced by the near-field chemistry (e.g., pH, chloride concentration, thermohydrologic conditions). The chemical changes of the water contacting the waste package (WP) are not modeled and the assumed environment does not correspond to bounding environments described in the DOE long-term testing program.

- Rationale for omitting potentially important container failure modes (i.e., stress corrosion cracking, crevice corrosion, thermal embrittlement of steel, and microbially influenced corrosion) is not provided in TSPA-95. Omitting these failure modes may lead to overestimation of WP lifetimes.

- The methodology lacks a mechanistic basis for considering the effect of galvanic coupling; this process could significantly extend container lifetimes.

4/51

Fracture/Matrix Interactions

- The conceptual model for flow and transport in the unsaturated zone lead to a very small fraction of transport through fractures or fast flow paths. Support for this conceptual model from experimental or field data is not provided. In the absence of such support, the transport result are not bounding.

Volcanism Scenario (direct releases)

- The TSPA-95 did not explicitly address the impact of volcanic eruptions on overall performance. Omission of disruptive scenarios should be based on demonstration of negligible effects or included in the assessment.

- A preliminary analysis conducted for the detailed review suggests that direct releases via magmatic extrusion and airborne transport could be significant to overall performance, depending on the particle size characteristics and the extent of waste incorporated in the ash material.

General findings and recommendations for improving the defensibility of future TSPAs in these specific areas are presented in this report.

5/51

CONTENTS

CONTENTS (Cont'd)

Section | Page

7/51

FIGURES

8/51

TABLES

Table | Page

ACKNOWLEDGMENTS

This report was prepared to document work performed by the Center for Nuclear Waste Regulatory Analyses (CNWRA) for the Nuclear Regulatory Commission (NRC) under Contract No. NRC-02-93-005. The activities reported here were performed on behalf of the NRC Office of Nuclear Material Safety and Safeguards, Division of Waste Management. The report is an independent product of the CNWRA and does not necessarily reflect the views or regulatory position of the NRC.

CNWRA staff contributing to the report include R.G. Baca, G.A. Cragnolino, B.E. Hill, M.S. Jarzemba, S. Mohanty, and W.M. Murphy. In addition, T. Ahn of the NRC made technical contributions to this report. The editors wish to thank E.J. Bonano, S.A. Stothoff, and N. Sridhar for their technical reviews and B. Sagar for his programmatic review. The assistance of Ms. C. Garcia in preparation of the report is much appreciated and to B. Long, who provided a full range of expert editorial services in the preparation of the final document.

ANALYSES AND CODES: The Engineered Barrier System Performance Assessment Code (EBSPAC) Version 1.0 and ASHPLUME Version 1.0 were used in the analyses presented in this report. The EBSPAC code is currently under the software quality assurance procedure designated as the CNWRA Technical Operating Procedure (TOP)-018. The ASHPLUME code is currently being placed under the software control requirements of TOP-018.

QUALITY OF DATA: Sources of data used in the analyses presented in this report are from the existing technical literature and are cited at the end of each chapter.

10/51

1 INTRODUCTION

1.1 BACKGROUND

In late 1995, the U.S. Department of Energy (DOE) issued the third in a series of reports on total system performance assessments (TSPAs) for the proposed high-level waste (HLW) repository located at Yucca Mountain (YM), Nevada. This third iteration was documented in the report entitled "Total System Performance Assessment—1995: An Evaluation of the Potential Yucca Mountain Repository" (TRW Environmental Safety Systems, Inc., 1995a). The report, referred to hereafter as TSPA-95, presented the DOE performance assessment (PA) approach, assumptions, data, and principal findings of the evaluation. Overall system performance was quantified in the DOE report in terms of both cumulative release and peak dose.

Technical evaluation of the proposed repository in TSPA-95 is distinct from the previous DOE iteration, designated TSPA-93 (Wilson et al., 1994), in a number of respects. Some of the major differences are that the latest iteration (i) incorporates additional site data (e.g., U.S. Geologic Survey infiltration map); (ii) considers a different waste package (WP) design (e.g., multi-wall container, in drift emplacement), (iii) considers a variety of design options (e.g., thermal load, backfill, alternative corrosion model); and (iv) does not consider disruptive events such as seismicity, volcanism, and human intrusion. The current TSPA iteration also includes extensive use of detailed process and abstracted models. New abstracted models were developed for analyzing drift scale thermal-hydrologic behavior, waste package (WP) degradation, near-field unsaturated zone aqueous flux, and unsaturated zone flow and transport.

In early 1996, the Center for Nuclear Waste Regulatory Analyses (CNWRA) conducted an audit review (Baca and Brient, 1996) of the DOE TSPA-95 in accordance with the Nuclear Regulatory Commission (NRC) Overall Review Strategy (Johnson, 1993). The audit review examined all of the report, but chose to stress the following five topics:

- Temperature and relative humidity calculations
- Container lifetime and source term
- Infiltration and deep percolation
- TSPA model abstractions
- Groundwater dilution

The audit review identified a number of significant potential vulnerabilities in the DOE TSPA-95 primarily associated with unsupported assumptions, unverified model abstractions, and use of parameter values, unsupported by field data. Specific recommendations for improving the defensibility of the analyses were made to the DOE and their support contractors. These recommendations were presented and discussed at a technical exchange meeting on TSPA-95 held in May 1996 in Las Vegas, Nevada. In addition, the NRC transmitted the audit review report (Baca and Brient, 1996) to the DOE in July 1996 (Austin, 1996). These comments were considered by the DOE in developing the TSPA-Viability Assessment Plan (TRW Environmental Safety Systems Inc., 1996).

11/51

This detailed review examines several of the technical concerns expressed, some of which were identified in the audit review of TSPA-95. Due to resource constraints, it was decided that this review should address a limited number of focus topics. Initially, six focus topics were selected for the Detailed Review of TSPA-95: (i) container lifetime, (ii) percolation flux, (iii) fracture/matrix interactions (i.e., matrix diffusion effects), (iv) faulting scenario (i.e., impacts on WPs), (v) volcanism scenario, and (vi) TSPA abstractions (i.e., propagating the effects of container lifetimes, percolation flux, and matrix diffusion). Of the detailed analyses conducted for these six focus topics, only three produced results with significant differences from TSPA-95 that merit transmittal to the DOE. The three topics addressed in this report are container lifetime, fracture/matrix interactions, and volcanism scenario.

The topics not discussed in this report include percolation flux, faulting scenario, and TSPA abstractions. These topics are viewed as important to performance and are being addressed in on-going technical analyses. The analysis of initial percolation flux models and assumptions in TSPA-95 did not identify concerns of a significant nature; in addition, the DOE is currently revising the abstractions for percolation flux. Because of the importance of percolation flux to overall performance, however, future CNWRA work will address this topic and make it available to the DOE. Faulting impacts on WPs were investigated using a new scenario model but the analysis was not sufficiently conclusive in nature to communicate to the DOE at this time. After completion of some subsequent work, the technical basis and sensitivity results for the faulting scenario will be captured in a technical report. The Total-system Performance Assessment (TPA) Version 2 code (Wescott et al., 1995) was used to assess significance of differences in model abstractions and subsystem calculations. Calculations were performed considering alternate abstractions for unsaturated flow (i.e., bounding conditions for fracture/matrix interactions) and alternate container life cumulative distribution functions (i.e., NRC estimates versus TSPA-95 estimates). The TPA calculations of cumulative release for these two cases were not sufficiently sensitive to merit comment at this time. This focus topic will be re-examined [as part of the NRC Key Technical Issues (KTI) sensitivity analyses] using the TPA Version 3 code to quantify sensitivity with respect to peak dose. Findings from this work will be documented in the next NRC HLW Program Annual Progress Report.

Other topics not addressed in this report are concerns regarding radionuclide transport and coupled thermal-mechanical-hydrological processes. These topics were identified as future review topics in the letter from Austin to Milner (1996). Analyses for these topics were not pursued because of the NRC budget constraints required deferral of work under the Radionuclide Transport and Repository Design and Thermal-Mechanical Effects KTIs.

1.2 OBJECTIVES OF THE DETAILED REVIEW

The objective of this detailed review is to establish more clearly the NRC approach and/or position on most of the areas of concern identified in the TSPA-95 audit review. Detailed technical analyses were performed to quantify, as much as is possible, differences between the NRC and the DOE approaches and performance estimates.

1.3 NUCLEAR REGULATORY COMMISSION KEY TECHNICAL ISSUES

To conduct more effectively its prelicensing activities, the NRC refocused its regulatory program on ten KTIs. These KTIs, in table 1-1, were identified through a combination of (i) iterative performance assessment (IPA), (ii) systematic regulatory analysis of the Code of Federal Regulations (CFR) Title 10, Part 60 (10 CFR Part 60), (iii) review of the DOE draft Waste Containment and Isolation

12/51

Strategy (TRW Environmental Safety Systems, Inc., 1995b), and (iv) NRC staff understanding of geologic processes and events relevant to the YM site. Each of these KTIs encompasses a number of subissues that the NRC uses to guide its program and resolution of principal issues. At present, the NRC and the DOE have agreed on the potential significance of eight of the ten KTIs. The two KTIs where the DOE differs with the NRC are igneous activity (i.e., volcanism) and structural deformation and seismicity.

Technical activities conducted within these ten KTIs provide the bases for development of acceptance criteria for compliance determination and for interactions with the DOE and other parties the central objective being issue resolution (Federline et al., 1996).

Table 1-1. Ten Key Technical Issues

Title
Total System Performance Assessment and Integration
Igneous Activity (Volcanism)
Unsaturated and Saturated Flow Under Isothermal Conditions
Thermal Effects on Flow
Container Life and Source Term *(deferred)*
Structural Deformation and Seismicity
Evolution of the Near-Field Environment
Radionuclide Transport *(deferred)*
Repository Design and Thermal-Mechanical Effects *(deferred)*
Activities Related to Development of the U.S. Environmental Protection Agency Yucca Mountain Standard

1.4 REVIEW APPROACH

The review topics were chosen because of their potential importance to the overall system performance and because the NRC and the CNWRA staffs have performed significant technical studies on them. Each review topic was probed through the conjunctive use of simple and detailed process models, as well as through use of the NRC IPA Phase 2 computer code (Wescott et al., 1995), and more recently developed performance assessment modules. These detailed review analyses were documented in a manner that will permit the DOE to understand the NRC approaches used in compliance determination.

1.5 REFERENCES

Austin, J.H. 1996. *Transmittal of the Results of the U.S. Nuclear Regulatory Commission Audit Review of the U.S. Department of Energy's 1995 Total System Performance Assessment.* Transmittal Letter July 10, 1996 to R.A. Milner, U.S. Department of Energy. Washington, DC: Nuclear Regulatory Commission.

Baca, R.G., and R.D. Brient. 1996. *Total System Performance Assessment 1995 Audit Review.* Letter Report. San Antonio, TX: Center for Nuclear Waste Regulatory Analyses.

Federline, M.V., R.L. Johnson, and J.T. Greeves. 1996. NRC's refocused prelicensing high-Level waste regulatory program. *Proceedings of the Seventh Annual International Conference on High-Level Radioactive Waste Management.* La Grange Park, IL: American Nuclear Society: 196–198.

Johnson, R.L. 1993. *Overall Review Strategy for the Nuclear Regulatory Commission's High-Level Waste Repository Program.* NUREG-1323, Rev 0, Washington, DC: Nuclear Regulatory Commission.

TRW Environmental Safety Systems, Inc. 1995a. *Total System Performance Assessment—1995: An Evaluation of the Potential Yucca Mountain Repository.* B00000000-01717-2200-00136. Las Vegas, NV: TRW Environmental Safety System, Inc.

TRW Environmental Safety Systems, Inc. 1995b. *Strategy for Waste Containment and Isolation for the Yucca Mountain Site.* Las Vegas, NV: TRW Environmental Safety Systems, Inc.

TRW Environmental Safety Systems, Inc. 1996. *Total System Performance Assessment—Viability Assessment (TSPA-VA).* Las Vegas, NV: TRW Environmental Safety Systems, Inc.

Wescott, R.G., M.P. Lee, N.A. Eisenberg, T.J. McCartin, and R.G. Baca. 1995. *NRC Iterative Performance Assessment Phase 2.* NUREG-1464. Washington, DC: Nuclear Regulatory Commission.

Wilson, M.L., J.H. Gauthier, R.W. Barnard, G.E. Barr, H.A. Dockery, E. Dunn, R.R. Eaton, D. C. Guerin, N. Lu, M.J. Martinez, R. Nilson, C.A. Rautman, T.H. Robey, B. Ross, E.E. Ryder, A.R. Schenker, S.A. Shannon, L.H. Skinner, W.G. Halsey, J.D. Gansemer, L.C. Lewis, A.D. Lamont, I.R. Triay, A. Meijer, and D.E. Morris. 1994. *Total-System Performance Assessment for Yucca Mountain—SNL Second Iteration (TSPA-93).* Albuquerque, NM: Sandia National Laboratories. SAND93-2675. Vols. 1 & 2.

14/51

2 KEY TECHNICAL ISSUE: CONTAINER LIFE AND SOURCE TERM

2.1 SCOPE OF REVIEW

The portions of TSPA-95 relevant to the Container Life and Source Term KTI concerning the prediction of container life over long periods in the environment of the proposed YM repository are identified in table 2-1.

Table 2-1. Total System Performance Assessment 1995 scope of review for the Key Technical Issue: Container Life and Source Term

Section	Title
3.5	Waste Package Design
3.6	Waste Package Emplacement
5	Waste Package Degradation Abstraction
5.1	Introduction
5.2	Corrosion Modes
5.3	Humid Air Corrosion Models for Corrosion-Allowance Materials
5.4	Aqueous Corrosion Models for Corrosion-Allowance Materials
5.5	Corrosion Modeling of Corrosion-Resistant Materials
5.6	Cladding Degradation
5.7	Waste Package Degradation History
5.8	Summary and Recommendations

2.2 AREA OF CONCERN: CONTAINER LIFETIME

2.2.1 Description of the Total System Performance Issue

The current conceptual design of the WP for spent fuel (SF) and vitrified defense high-level waste (DHLW) (TRW Environmental Safety Systems, 1996) was evaluated in TSPA-95 (TRW Environmental Safety Systems, 1995a) using a stochastic WAste Package DEGradation (WAPDEG) code Version 1.0 (Atkins and Lee, 1996). Although the Advanced Conceptual Design Report (ACDR) (TRW Environmental Safety Systems, 1996) was not available at the time that TSPA-95 was conducted, the design related input used in TSPA-95 (TRW Environmental Safety Systems, 1995b) differs only slightly from that reported in the ACDR. The ACDR design is a significant departure from the single-wall container concept evaluated in TSPA-93 (Wilson et al., 1994). It consists of an outer disposal overpack made of a corrosion-allowance material (carbon steel) and an inner container made of corrosion-resistant material Alloy 825 (this may be changed to Alloy 625 in the TSPA-VA). An additional containment

15/51

barrier of a moderately corrosion-resistant material such as Alloy 400 was included in the low thermal load repository design (TRW Environmental Safety Systems, 1994). This additional containment barrier was not considered in TSPA-95 based on the argument that models for predicting the performance of this type of material are not currently available. Also, the multi-purpose canister (MPC) made of type 316L stainless steel and the pour canister for DHLW are not included in TSPA-95, since no credit is presently assigned by the DOE to these canisters as containment barriers. Cladding degradation processes are briefly discussed in section 5.6 of TSPA-95; however, evaluation of the performance of fuel cladding as potential barrier is not included.

Although several corrosion modes (i.e., crevice corrosion, stress corrosion cracking, microbially influenced corrosion, and galvanic corrosion) are briefly mentioned in an introductory discussion (TSPA-95, pp. 5-2 and 5-3) as potential failure modes for the WP, the performance calculations in TSPA-95 include only general corrosion and pitting corrosion. Additional calculations are also included to demonstrate that the carbon steel outer barrier can provide corrosion protection to the Alloy 825 inner container through galvanic coupling. Air oxidation of canister material is considered negligible, but concern about the corrosion-resistance of welds is noted.

While there are certain conservatisms in the TSPA-95 WP performance analyses, there are some assumptions that may lead to nonconservative results

- The evolution of the environment chemistry contacting the WP is not modeled and the assumed environment does not correspond to bounding environments described in the DOE long-term testing program (McCright, 1995)

- Rationale for omitting failure modes, such as stress corrosion cracking, microbially influenced corrosion, thermal embrittlement of steel, and crevice corrosion, is not provided and their omission may lead to overestimation of WP lifetimes

2.2.2 Description of the U.S. Department of Energy Approach and/or Position

In general terms, the approach adopted in TSPA-95 regarding WP degradation is consistent with the hypothesis on waste containment presented in the document on the DOE Waste Containment and Isolation Strategy for the Yucca Mountain Site (TRW Environmental Safety Systems, 1995c). In particular, the WP environment in both documents is assumed to be humid air at elevated temperatures.

In the TSPA-95 report, humid air corrosion is considered to be corrosion that takes place under a thin film of water that forms on the container surface above a critical relative humidity range uniformly distributed between 65 and 75 percent. Aqueous corrosion refers to corrosion of metal in contact with bulk water, assumed to occur at relative humidities greater than a threshold value uniformly distributed between 85 and 95 percent.

The model for humid air corrosion of the outer steel container is based on assuming an exponential dependence of the corrosion rate with the relative humidity (RH), the inverse of absolute temperature (T), and the concentration of SO_2 in the environment (SO_2). In addition, a power dependence of the general corrosion depth (D_g^h) with time (t), leads to the following empirical expression:

16/51

$$\ln D_g^h = a_0 + a_1 \ln(t) + a_2/RH + a_3/T + a_4[SO_2] + \epsilon \tag{2-1}$$

The parameters a_i in Eq. (2-1) were obtained from linear regression of 166 data points acquired from atmospheric corrosion exposures in different locations (tropical, rural, urban, and industrial sites, with the exclusion of marine sites) extended to a total of 16 yr using a specific equation to account for the time fraction during which the RH was greater than 70 percent. The term ϵ represents uncertainties not explained by the model. Pitting corrosion was treated as an uncertainty by using a pitting factor to obtain pit depth from the general corrosion penetration in humid air. On the basis of inland tropical environment corrosion testing data, the pitting factor was assumed to be normally distributed with a mean of 4.0 and a standard deviation of 1.0. In addition, the pitting factor was constrained to be equal or greater than 1.0. Pitting initiation was not explicitly considered and therefore pits were assumed to grow as soon as general corrosion starts.

An expression similar to Eq. (2-1) was used in TSPA-95 (5–14) for general corrosion of the outer steel container under aqueous conditions

$$\ln D_g^a = b_0 + b_1 \ln(t) + b_2/T + b_3 T^2 + \epsilon \tag{2-2}$$

The parameters b_i in Eq. (2-2) were obtained from long-term (to 16 yr) corrosion data acquired in polluted river water and tropical lake water combined with short-term (100 d) corrosion data from distilled water to deduce the temperature effect. As in the case of the humid air environment, pitting corrosion was evaluated from general corrosion calculations by using a pitting factor with the values noted previously.

Humid air corrosion and general corrosion in the aqueous environment were assumed in TSPA-95 to be negligible for the inner corrosion-resistant container. The pit growth rate for pitting corrosion in an aqueous environment, assumed to be a function of temperature only was expressed as

$$\ln R_p = 50.373 - \frac{19655.85}{T} \tag{2-3}$$

where R_p is a median pit growth rate in mm/yr and T is temperature in °K.

By using temperature and humidity profiles at the WP surface obtained from drift-scale thermohydrologic modeling and Eqs. (2-1) through (2-3), stochastic simulations of WP degradation were performed using the WAPDEG code. Simulations were also conducted to evaluate the effect of WP cathodic protection by assuming that pitting corrosion of the corrosion resistant inner barrier would be delayed until the thickness of the carbon steel outer barrier is reduced by 75 percent.

The adequacy of the data used in TSPA-95 to obtain the values of the coefficients in Eqs. (2-1) and (2-2), as well as the use of simple power laws to express the time dependence and linear regression fits for long-term predictions, were questioned in the audit review (Baca and Brient, 1996).

2.2.3 Detailed Review Approach

A detailed evaluation of specific failure processes, including sensitivity analyses, was performed by the NRC and the CNWRA staffs to assess methodologies used by the DOE in TSPA-95. Container life cumulative distribution curves were obtained using the Engineering Barrier System Performance Assessment Code (EBSPAC) Version 1.0 (Mohanty et al., 1996) and compared with those obtained by using WAPDEG Version 1.0 (Atkins and Lee, 1996).

2.2.3.1 Sensitivity Analyses

This section presents the NRC approach to sensitivity analyses of WP performance through the use of EBSPAC. Sensitivity analyses were conducted to evaluate the relative importance of certain processes and the associated variables or parameters on the performance of WPs. Detailed conceptual and numerical models adaptable to the conditions prevailing in a repository under partially saturated conditions exist for many corrosion and mechanical failure processes. Material specific parameters for some of these models however are scarce. For this analysis, values for these parameters were obtained through reviews of published literature and information reported by the DOE, combined with data obtained in the experimental investigations program conducted within the Container Life and Source Term KTI.

For the EBSPAC calculations, only the WP designed for 21 PWR or 40 BWR SF assemblies in a horizontal drift emplacement, as currently envisioned by the DOE (TRW Environmental Safety Systems, Inc., 1996), was considered. As a set of external calculations to EBSPAC, a conduction-only thermal model provides temperature distribution as a function of time and position within the Engineered Barrier System (EBS) as well as in the surrounding geosphere (Manteufel, 1996). Values of parameters such as temperature and RH at the WP surface are calculated as functions of time by the thermal model and used to predict the occurrence and rate of corrosion of the WP and the subsequent release of radionuclides. The near-field environment model, MULTIFLO (Lichtner and Seth, 1996), was used to determine the chemical composition and pH of the aqueous solution able to contact the WP. MULTIFLO considers the evaporation and condensation associated with heat generated by radioactive decay, in conjunction with transport of reactive constituents involving two-phase fluid flow.

Below a critical value of RH, air oxidation of steel is modeled as the dominant corrosion process for the steel overpack. The possibility of mechanical failure as a result of thermal embrittlement of the steel promoted by long-term exposure to temperatures above 150 °C is evaluated at each time step. If the RH is higher than the critical value, the occurrence of aqueous corrosion of the steel overpack is evaluated. No distinction is made in EBSPAC between humid air corrosion and aqueous corrosion because both processes are governed by the same fundamental electrochemical mechanisms.The corrosion process at any given time depends on the corrosion potential and the critical potential required to initiate a particular localized corrosion process. In this analysis, the repassivation potential, E_{rp}, is conservatively adopted as the critical potential for the initiation of localized corrosion. If the corrosion potential is higher than the repassivation potential, it is assumed that localized corrosion is initiated without an induction time; if not, uniform corrosion under passive conditions takes place. Corrosion models calculate rates of uniform and localized corrosion. Following penetration of the outer container, electrical contact of the inner and outer container through the presence of an electrolyte path (such as that provided by modified groundwater) promotes galvanic coupling, assuming that metallic contact always exists between both containers. The galvanic coupling model evaluates whether penetration of the inner container by localized

18/51

corrosion is possible; if not, uniform corrosion or mechanical fracture becomes the predominant failure mechanism because the inner container is protected against localized corrosion.

Calculations were performed to examine the effect of galvanic coupling on the failure time of the WP. A simplified approach is used to account for galvanic coupling effects between the inner and the outer overpacks. The corrosion potential of the galvanic couple formed when the wall of the outer container is penetrated by a pit, E_{corr}^{wp}, is estimated by using experimentally measured values of the potential of the bimetallic couple, E_{corr}, for a well-defined area ratio between both components. The E_{corr}^{wp} is determined through a linear combination of E_{corr} of the inner overpack as calculated at the time of through-wall penetration of the outer container and E_{couple} according to the following empirical expression

$$E_{corr}^{wp} = (1-\eta)\ E_{corr} + \eta\ E_{couple} \tag{2-4}$$

where η is the efficiency of the galvanic coupling with the condition $0 \le \eta \le 1$. A value of E_{couple} equal to $-0.46\ V_{SHE}$ was adopted on the basis of results reported by Scully and Hack (1984) for a galvanic couple made of steel and Alloy 625 (a nickel-base alloy similar in electrochemical behavior to Alloy 825) with an area ratio 1:1 and exposed to sea water. The values adopted for the different parameters needed to calculate E_{corr} and those establishing the dependence of the critical potentials with chloride concentration and temperature are reported elsewhere (Mohanty et al., 1996). Based on near-field simulation using the MULTIFLO (Lichtner and Seth, 1996) code, a chloride concentration of 0.3 mol/L was used for temperatures above the boiling point of water; below the boiling point of water, a value of 3×10^{-3} mol/L was used. For localized corrosion, no initiation time is assumed if E_{corr}^{wp} is greater than E_{rp}. If this condition is satisfied, a constant value of $6.3\times10^{6}\ cm^{-2}\ yr^{-1}$ ($2\times10^{-5}\ A/cm^2$) is used for the pit propagation rate of the inner overpack material, which represents values typical of slow active dissolution (Mohanty et al., 1996).

Figure 2-1 shows the calculated WP failure time as a function of the galvanic coupling efficiency (η) for three values of the areal mass loading (AML), currently a repository design variable. The calculations correspond to the thermal model cases (Mohanty et al., 1996) in which no ventilation occurs during the initial 100 yr operations period and with no backfill after permanent closure. It is seen that at 80 MTU/acre, which is close to the value adopted in TSPA-95 for the high thermal loading case, η has an important effect on the WP failure time which increases abruptly from 2,736 yr to more than 10,000 yr (the simulation time) for η values close to 0.2. A similar effect is observed at 40 MTU/acre where failure time increases from 472 yr to more than 10,000 yr for η values just above 0.08. On the contrary, at 20 MTU/acre, failure time is always greater than 10,000 yr regardless of the value of η. If galvanic coupling is completely ineffective ($\eta = 0$), the shortest failure time occurs at the intermediate AML (40 MTU/acre). The wetting time is also the shortest at the intermediate AML, but the differences in failure times are only explainable by the effect of temperature on the initiation of localized corrosion. The wetting times, corresponding to a critical value of RH equal to 65 percent, are 153, 50, and 2,336 yr for 20, 40, and 80 MTU/acre.

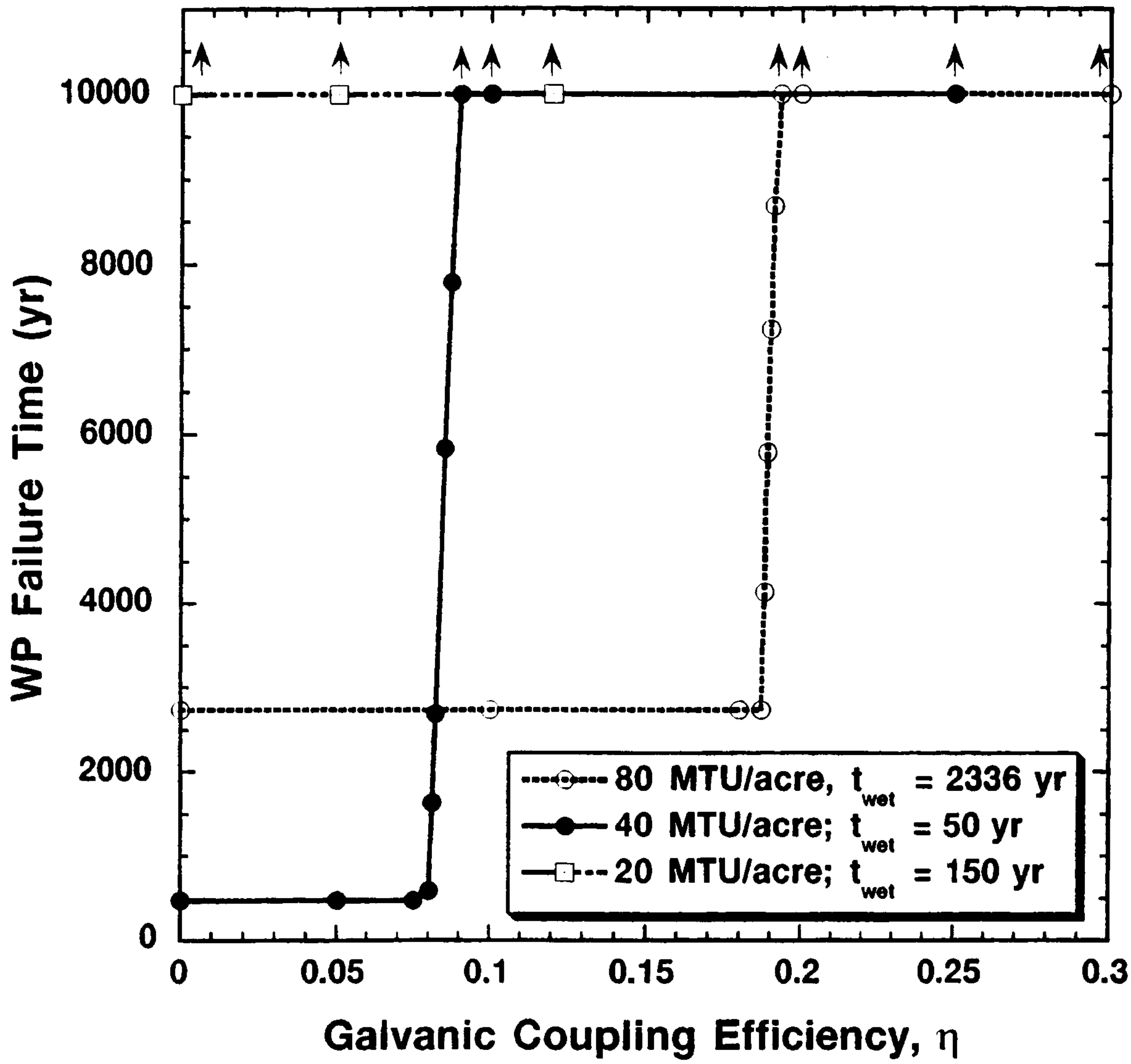

Figure 2-1. Effect of galvanic coupling on the waste package failure time for two values of areal mass loading in the absence of ventilation and backfilling. Arrows denote failure times greater than 10,000 yr.

Although penetration by localized corrosion of the outer container occurs in a few hundred years, only slow passive dissolution of the inner Alloy 825 container takes place subsequently for 20 MTU/acre because E_{corr} is lower than the critical potential for localized corrosion at the relatively low temperatures encountered at this low AML. In this case, the inner container fails just after 10,000 yr. In summary, the critical potential above which localized corrosion occurs increases with a decrease in temperature so the likelihood of localized corrosion for a given chemical environment decreases with a decrease in AML. At high AML, WP remains dry for a long period and the container life is long. These two competing factors lead to a minimum container life at an intermediate AML. If efficient galvanic coupling occurs, container life can be greater than 10,000 yr, independent of the AML value.

With ventilation during the operation period and backfill material after closure, the calculated failure time is longer than 10,000 yr at low values of AML, as shown in figure 2-2, regardless of the effect of galvanic coupling. At 80 MTU/acre the WP life increases from 2,636 to more than 10,000 yr as a result of effective galvanic coupling $(\eta = 1)$. The wetting times decrease with increasing AML in the presence of ventilation and backfilling, as presented in figure 2-2.

Additional sensitivity analyses include the effect on WP lifetime of varying several parameters of interest such as chloride concentration and critical RH, among others. Several factors can decrease the critical RH required to form a multilayer film of water on WP surfaces (Mohanty et al., 1996). Capillary condensation of water can occur in the pores of a preformed oxide or oxyhydroxide layer and at interstices formed by air-borne particles or particles of backfill material with the WP surface. In addition, the deposition of hygroscopic salts on the metal surface can substantially decrease the critical RH required to form a water film. All these factors can lead to a substantial decrease of the threshold RH and therefore to the occurrence of uniform or localized corrosion at shorter times. The critical RH can be as low as 48 percent for the capillary condensation of water at pores with a radius of 1.5 nm as calculated at 100 °C by using the Thomson (Lord Kelvin) equation. In addition, the RH of air in equilibrium with a NaCl saturated solution decreases to 76 percent of that of pure water (Fyfe, 1994). Considering these two factors, the actual critical RH value can be as low as 36 percent. Preliminary EBSPAC calculations using a critical RH uniformly distributed between 35 to 55 percent, instead of 55 to 75 percent used in most simulations, reduced the container life to about 1,000 yr.

2.2.3.2 Thermal Embrittlement of Carbon Steel

Depending upon the DOE thermal loading strategy, WP materials can be exposed to temperatures well above 100 °C for thousands of years. In addition, backfilling can induce a sharp increase in temperature of the WP surface above 100 °C followed by a gradual decrease with time. In TSPA-95 (TRW Environmental Safety Systems, Inc., 1995a), no consideration was given to the effect of prolonged exposures at these temperatures on material stability. Specific mechanical properties such as fracture toughness may be degraded under such conditions causing embrittlement. Thermal embrittlement is related to the well-known phenomenon of temper embrittlement that affects tempered low-alloy steels as a result of isothermal heating or slow cooling within the temperature range of 325 to 575 °C. Temper embrittlement is a major concern to the integrity of engineering components that operate within that critical temperature range and also to heavy section components slowly cooled through the critical temperature range after heat treatment or welding operations.

Based on review of the literature (Cragnolino et al., 1996), it was concluded that low-alloy steels, such as A387 Grade 22 (2.25 Cr-1Mo Steel), and possibly C-Mn steels, such as A516 Grade 55, may be susceptible to a substantial degradation in toughness as a consequence of long-term thermal aging at repository temperatures anticipated for high AMLs (i.e., >200 °C). The susceptibility to thermal embrittlement of some candidate materials for the WP outer disposal overpack can be reduced through appropriate selection of the steel chemical composition or processing techniques. The investigation also revealed that low-alloy steels are more susceptible to thermal embrittlement than plain carbon steels. Therefore, it is preferable to use plain carbon steels if thermal embrittlement is a matter of concern at high AMLs. It is however preferable to use low-alloy steels to resist humid air and aqueous corrosion, which may become more significant under a low thermal loading strategy. Hence, selection of outer overpack must involve a balance between these considerations and the thermal loading strategy.

21/51

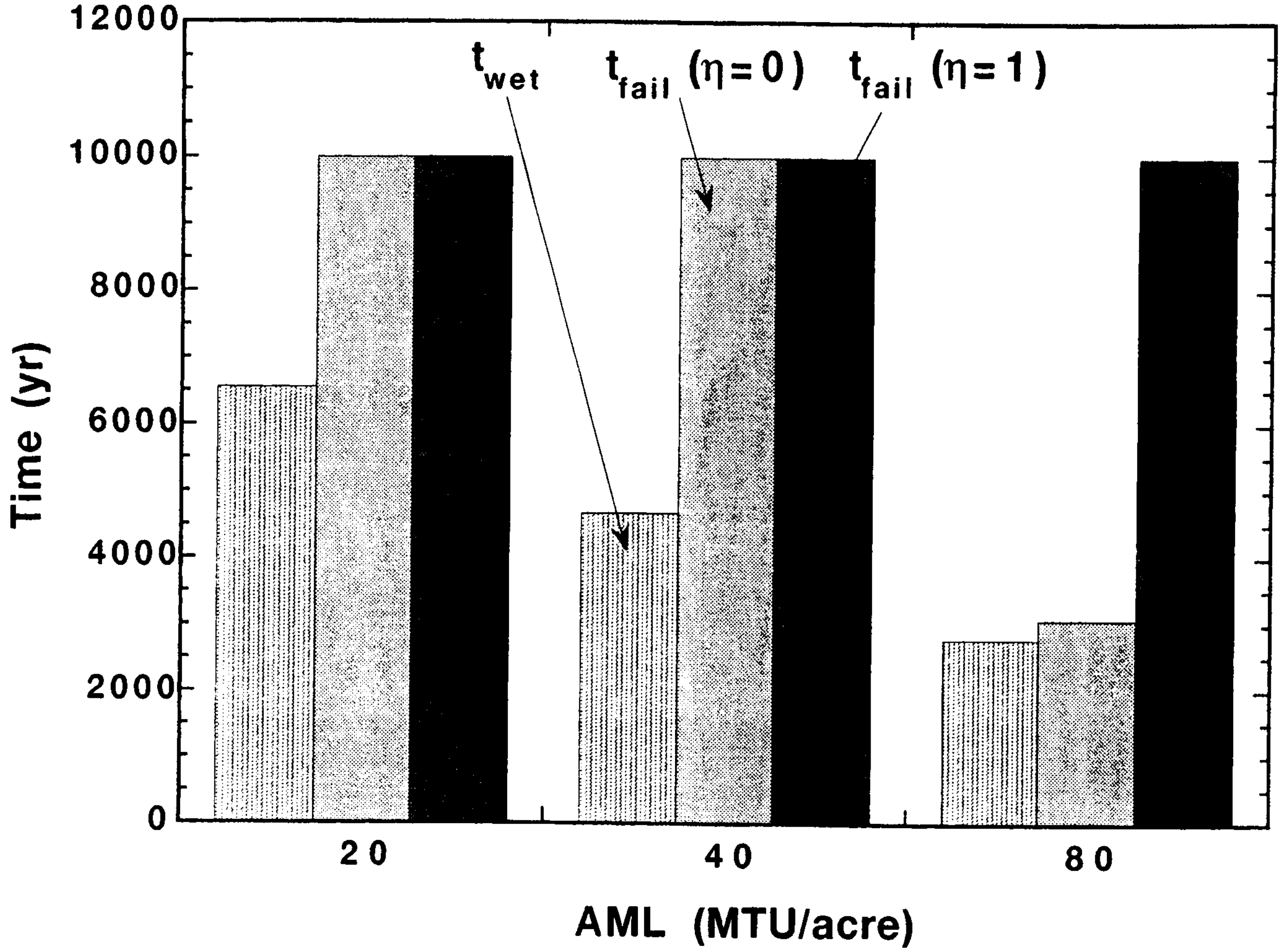

Figure 2-2. Waste package failure as a function of thermal loading, ventilation, and galvanic coupling effect in the presence of ventilation and backfilling after closure

In TSPA-95, the DOE did not address the potential for mechanical failure of the carbon steel overpack associated with thermal embrittlement. Preliminary calculations indicate that thermal embrittlement susceptibility could be significant only at WP temperatures exceeding 200 °C over extended periods (thousands of years). Sources of uncertainties in the degree of embrittlement related to uncertainties in models, parameters, or data have been identified, but additional work will be necessary following appropriate sensitivity analyses. A knowledge of detailed WP design parameters is necessary to address this issue quantitatively.

22/51

2.2.3.3 Dry Oxidation of Carbon Steel

Under dry conditions corresponding to RHs lower than the critical value, one potential degradation mode of the outer steel container is dry oxidation caused by chemical reaction with gaseous oxygen in air at temperatures well above 100 °C. The formation of an oxide layer with uniform penetration in the metal of 2 μm after 10,000 yr at 200 °C has been predicted by the DOE (Stahl and McCoy, 1995). More recently, Henshall (1996) predicted, by assuming a parabolic growth law, a penetration of 127 μm after exposure to temperatures decreasing from 280 to 210 °C during 5,000 yr.

Larose and Rapp (1996) undertook a detailed examination of the potential for dry oxidation at repository temperatures of carbon and low alloy steels. At temperatures below 567 °C, the oxide scale is formed by two layers, an inner layer composed of magnetite (Fe_3O_4) and the outer layer of hematite (Fe_2O_3). The oxidation rate of steel at low temperatures increases with the carbon content of the steel. At 250 °C carbon steels containing 0.2 weight percent carbon are expected to lose about 4 μm in thickness after 1,000 yr (approximately 13 μm in 10,000 yr). They concluded that because low temperature oxidation in carbon and low alloy steels followed a parabolic law and are controlled by outward diffusion of iron rather than inward diffusion of oxygen, intergranular penetration of oxide would not be significant. Also, no breakaway of the kinetics can be expected within 10,000 yr even at 300 °C because the oxide layer is relatively thin to be undermined by internal stresses.

Ahn (1996) estimated a 90 μm penetration after 10,000 yr at 200 °C through extrapolations of grain boundary oxidation at 600 °C. He suggests that localized oxidation may take place in the form of oxide islands or grain boundary oxides even at relatively low temperatures on the basis of observations of grain boundary oxidation in Fe-2.25Cr-1Mo at 550 °C after 6 h (Raman et al., 1992) and in Fe-10Cr-34Ni at 600 °C after 1,000 h (Newcomb and Stobbs, 1991). Ahn (1996) predicted a much deeper and localized penetration of oxide because of grain boundary diffusion of oxygen. If oxygen diffusion controls low temperature oxidation, grain boundary oxidation would be promoted since diffusion along grain boundaries is several orders of magnitude faster than in the matrix. Considering that the ratio between grain boundary and matrix diffusivity could be as high as 10^5 at 1,000 °C, an even larger ratio is suggested at repository temperatures, making necessary a further assessment of the possibility of intergranular oxidation (Ahn, 1996). It is suggested that the localized oxide can promote pit propagation or act as a flaw leading to early mechanical failure arising from its brittle nature.

Different interpretations have been developed regarding the mechanisms of dry oxidation of steels (Ahn, 1996; Henshall, 1996; Larose and Rapp, 1996) which lead to different values of oxide penetration by extrapolating high temperature data. This is a subissue that may require further evaluation of the literature or focused experiments for resolution.

2.2.3.4 Long-Term Aqueous Corrosion Prediction

Modeling of the evolution of the near-field environment has shown saturation increases above and below the repository horizon and saturated zone water is alkaline. Such conditions promote passivation of carbon steels (Pourbaix, 1974). When steel exhibits passive behavior, the presence of low concentrations of chloride in the groundwater however can induce localized attack (pitting or crevice corrosion) (Szklarska-Smialowska, 1986; Marsh et al., 1985) even though carbon steels are typically considered a corrosion-allowance material. Finally, the presence of micro-organisms can alter the local environment adjacent to the WP and accelerate the localized or uniform corrosion rate (Geesey, 1993).

It has been demonstrated by Fukuda and Akashi (1996) that in slightly alkaline environments containing chlorides, the occurrence of localized corrosion on carbon steels can be predicted using the same approach as that for corrosion-resistant materials such as alloy 825. Localized corrosion is assumed to initiate when the E_{corr} of the steel overpack is greater than the repassivation potential, E_{rp}. The CNWRA measured the E_{rp} of both A516 grade 60 carbon steel, which is similar to the candidate outer overpack material, and Alloy 825, a candidate inner overpack material, in a wide range of chloride containing solutions simulating the aqueous environments that may prevail at the repository site. The data generated from these tests are used in EBSPAC as input to the calculations to predict container life. Long-term testing of Alloy 825 accumulating over 900 d tends to confirm that E_{rp} is a conservative parameter for predicting localized corrosion.

Experimental work at the CNWRA on Microbially Induced Corrosion (MIC) demonstrated that localized corrosion of corrosion-resistant materials such as type 316L stainless steel can occur in the presence of bacteria such as *S. Putrefaciens*. The effect cannot be attributed to an increase in E_{corr} but to a decrease in E_{rp} that can be due to the concentration of metabolic products such as sulfide in localized areas of the metal surface. These results combined with observations reported by Pitonzo et al. (1996) regarding the existence of several species of bacteria responsible for MIC failures confirm the need for a complete assessment of the effects of MIC on WP failure.

2.2.3.5 Analyses of U.S. Department of Energy Cumulative Distribution Functions

EBSPAC was used to conduct an independent review of the container life cumulative distribution functions presented in TSPA-95. A total of 27 model input parameters were sampled from specified distributions using the Latin Hypercube Sampling method with most variabilities representing the uncertainties in the experimental data. Stochastic simulations with the EBSPAC were performed using 100 realizations. Three important parameters were kept constant and studied on a case-by-case basis: (i) temperature, (ii) corrosion rate due to uniform or localized corrosion, and (iii) galvanic coupling. Preliminary calculations clearly indicate that there are two parameters of greatest importance to container life: the AML, which in conjunction with the use of ventilation and backfilling, determines WP temperature, RH, and the chemical composition of the near-field environment; and the degree of galvanic coupling between the outer carbon steel overpack once it is breached and the inner nickel-base alloy overpack. This degree of galvanic coupling determines the failure time of the WP inner overpack. Limited sensitivity analyses indicate that uniform and localized corrosion rates are also important factors on WP life. Additional analyses are needed to completely assess the influence of other dominant environmental and materials factors on WP life.

The cumulative distribution of lifetimes with and without galvanic coupling, in the absence of ventilation and backfilling after closure, is presented in figure 2-3 for a value of AML equal to 80 MTU/acre. The failure distribution curves from TSPA-95 are compared with those from EBSPAC. In the absence of galvanic coupling, the percentage failure after 10,000 yr is greater for TSPA-95 calculations. However, a significant percentage of WP failures takes place between 2,000 and 3,000 yr in the EBSPAC calculation as compared to a more gradual increase in the percentage failure with time for TSPA-95. When effective galvanic coupling occurs, the WP percentage failure at 10,000 yr is significantly decreased and the first failure is delayed by nearly 3,000 yr in the curve representing EBSPAC results.

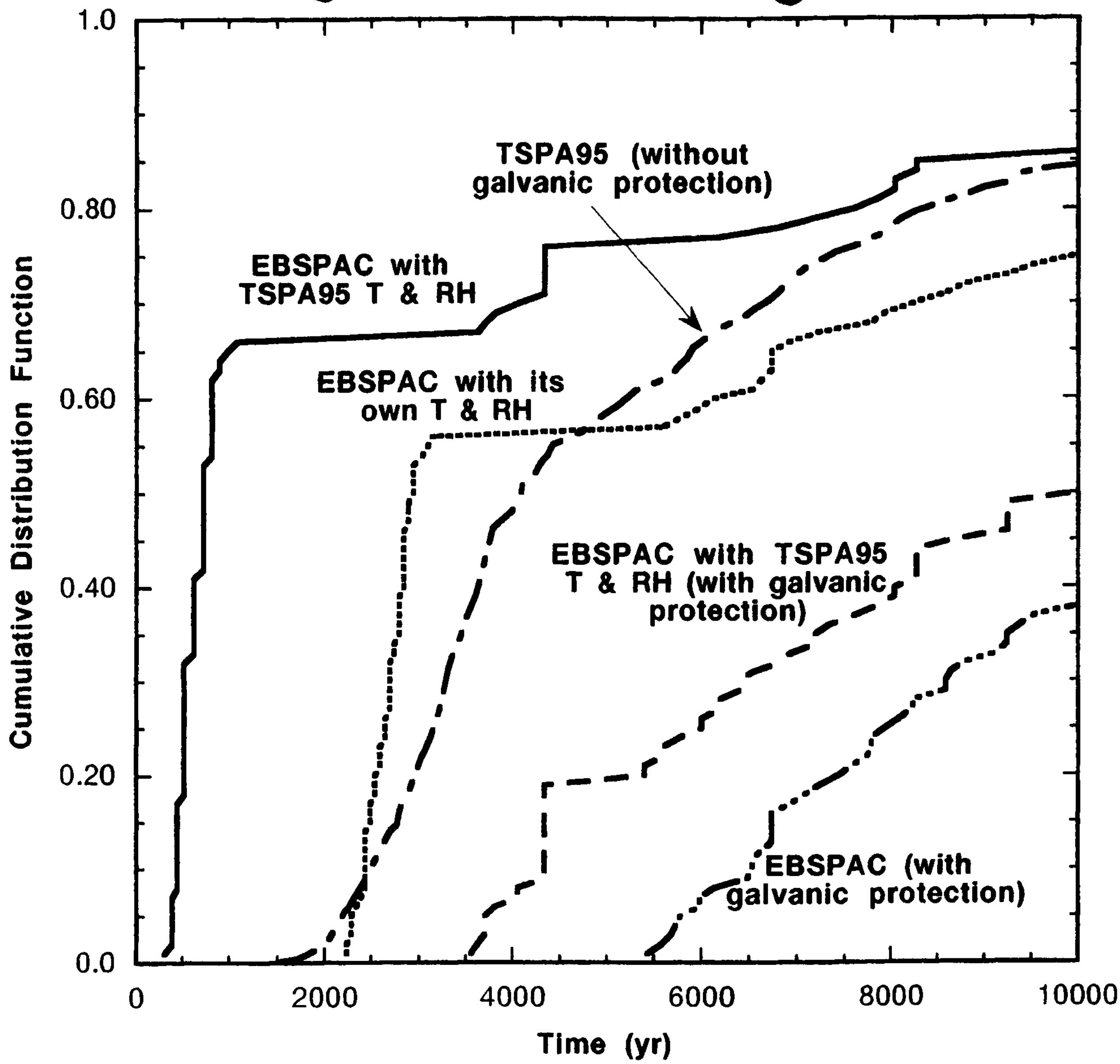

Figure 2-3. Comparison of Total System Performance Assessment—95 and Engineered Barrier System Performance Assessment Code cumulative distribution functions of waste package failure

A significant difference was noticed when temperature and RH predictions by the NRC and TSPA-95 were compared (Baca and Brient, 1996). If temperature and RH values in TSPA-95 are used as input to EBSPAC calculations, a significant difference in the WP failure time distribution is noticed. The results shown in figure 2-3 reveal that the WP lifetime after 10,000 yr is similar to that calculated in TSPA-95. However, the percentage of WP failures at all times remained higher than that predicted by the DOE. It is also shown that percentage of WP failure times with galvanic protection is always greater than that calculated by EBSPAC with TSPA-95 temperature and RH. These results indicate that temperature calculations should be realistically and accurately predicted because of their direct effect on WP degradation processes.

25/51

2.3 DESCRIPTION OF THE LIKELY EFFECTS ON PERFORMANCE

The corrosion models adopted in TSPA-95, as discussed previously, may lead to an overestimation of repository performance unless the models can be shown to be applicable to YM. The most important factor appears to be related to the selection of incomplete conceptual models (i.e., lack of consideration of several relevant corrosion failure modes). With the exception of thermal embrittlement, however, lack of consideration of other failure modes in the simulations of WP degradation, such as crevice corrosion, stress corrosion cracking, and microbially influenced corrosion, is acknowledged in the current iteration presented in TSPA-95 and can be addressed in future interactions with the DOE.

The TSPA-95 approach does not include models involving the interaction of engineering materials with the environment that are reasonably general (e.g., chemical species over a wide concentration range can not be represented and redox characteristics of the environment and effects on corrosion potentials of metallic materials can not be considered). This limitation may partly arise from the use of a restricted database for the determination of relevant equations and parameters involved in humid air and aqueous corrosion. Furthermore, the models used in TSPA-95 have inadequate mechanistic justification. The selection of an inadequate functional relationship may lead to significant differences with expressions more justifiable from fundamental principles of electrochemical corrosion, thermohydrology, and near-field chemistry when these models (and data obtained over a period of few years) are extrapolated to predict the behavior after thousands of years. Approaches to deal with this level of uncertainty are not presented in TSPA-95. The choice of pitting factors needs to be substantiated either in mechanistic models or by sufficient data. Pitting factors observed experimentally at Lawrence Livermore National Laboratory are much higher than four and under wet-dry conditions may be as high as 100. Underestimating uncertainty concerning corrosion models results in a lower probability of early container failure. In addition, a limited range of environmental conditions was considered in TSPA-95 (e.g., evaporative effects associated with radioactive decay, heat, or other local modifications of the environment were not examined).

The TSPA-95 analysis can be made more defensible by

- Including in the WAPDEG code (Atkins and Lee, 1996) a better description of the evolution of chemical composition and variables of the near-field environment affecting container life, such as pH and chloride concentration, as a function of temperature and time or use bounding values for such variables. Models defining the near-field environment at the drift scale using coupled thermo-hydrological-chemical calculations may be abstracted and used in codes for evaluating WP performance.

- Developing a mechanistic basis for the description of corrosion during wet/dry periods, including the consideration of changes on WP surface (e.g., porous deposits) that may affect the critical value of RH required for humid air corrosion (Mohanty et al., 1996) or verifying empirical model with a sufficient amount of data.

- Using a mechanistic approach to pitting corrosion and choosing a more conservative parameter than the pit initiation or nucleation potential to predict its occurrence.

- Developing a better technical basis for consideration of galvanic coupling.

In addition, it would be beneficial if the DOE program (i) addresses uncertainties associated with potential effects of micro-organisms in the near-field environment and on container failure and (ii) evaluates the potential for localized dry oxidation and thermal embrittlement of the steel outer overpack while taking into consideration thermal loading strategy and detailed design of WPs.

2.4 REFERENCES

Ahn, T.M. 1996. *Dry Oxidation of Waste Package Materials*. NUDOC Accession Number: 9607290014. Washington, DC: Nuclear Regulatory Commission.

Atkins, J.E., and J.H. Lee, 1996. *Waste Package Degradation (WAPDEG) Simulation Code*. Version 1.0 (Preliminary Draft) Las Vegas, NV: INTERA.

Baca, R.G., and R.D. Brient. 1996. *Total System Performance Assessment 1995 Audit Review*. Letter Report. San Antonio, TX: Center for Nuclear Waste Regulatory Analyses.

Cragnolino, G.A., H.K. Manaktala, and Y-M. Pan. 1996. *Thermal Stability and Mechanical Properties of High-Level Radioactive Waste Container Materials: Assessment of Carbon and Low-Alloy Steels*. CNWRA 96-004. San Antonio, TX: Center for Nuclear Waste Regulatory Analyses.

Fukuda, T., and M. Akashi. 1996. Effect of $[HCO_3^- + CO_3^{2-}]$ on Corrosion Crevice Repassivation Potential of Carbon Steel in Simulated Bentonite Environment. *Scientific Basis for Nuclear Waste Management XIX—Symposium Proceedings*. W.M. Murphy and D.A. Knecht, eds. Pittsburgh, PA: Materials Research Society 412: 597–602.

Fyfe, D. 1994. *Corrosion*. R.A. Jarman and G.T. Burstein, eds. Oxford, United Kingdom: Butterworths Heinmann: 1: 2:31–2:42.

Geesey, G. 1993. *A Review of the Potential for Microbially Influenced Corrosion of High-Level Nuclear Waste Containers*. G. Cragnolino, ed. CNWRA 93-014. San Antonio, TX: Center for Nuclear Waste Regulatory Analyses.

Henshall, G.A. 1996. Numerical predictions of dry oxidation of iron and low-carbon steel at moderately elevated temperatures. *Scientific Basis for Nuclear Waste Management XX Symposium Proceedings*. Pittsburgh, PA: Materials Research Society. To be published.

Larose, S., and R.A. Rapp. 1996. *Review of Low-Temperature Oxidation of Carbon Steels and Low-Alloy Steels for Use as High-Level Radioactive Waste Package Materials*. San Antonio, TX: Center for Nuclear Waste Regulatory Analyses.

Lichtner, P.C., and M.S. Seth. 1996. *User's Manual for MULTIFLO: Part II—MULTIFLO 1.0 and GEM 1.0, Multicomponent-Multiphase Reactor Transport Model*. CNWRA 96-010. San Antonio, TX: Center for Nuclear Waste Regulatory Analyses.

McCright, R.D. 1995. *Scientific Investigation Plan for Yucca Mountain Project (YMP) WBS Element 1.2.2.5.1. Metal Barrier Selection and Testing*. SIP-CM-01 Rev. 2. Livermore, CA: Lawrence Livermore National Laboratory.

Manteufel, R.D. 1996. Effects on ventilation and backfill on a mined waste disposal facility. *Nuclear Engineering and Design*. Submitted for publication.

Marsh, G.P., K.J. Taylor, I.D. Bland, C. Wescott, P.W. Tasker, and S.M. Sharland. 1985. Evaluation of localized corrosion of carbon steel overpacks for nuclear waste disposal in granite environments. *Scientific Basis for Nuclear Waste Management IX Symposium Proceedings*. L.W. Werme, ed. Pittsburgh, PA: Materials Research Society 59: 421–428.

Mohanty, S., G.A. Cragnolino, T. Ahn, D.S. Dunn, P.C. Lichtner, R.D. Manteufel, and N. Sridhar. 1996. *Engineered Barrier System Performance Assessment Code: EBSPAC Version 1.0 β, Technical Description and User's Manual*. CNWRA 96-011. San Antonio, TX: Center for Nuclear Waste Regulatory Analyses.

Newcomb, S., and W. Stobbs. 1991. The effects of a grain-boundary on the compositional fluctuations inherent in the oxidation of Fe-10Cr-34Ni. *Oxidation of Metals* 35: 69–88.

Pitonzo, B., P. Castro, P. Amy, D. Bergman, and D. Jones. 1996. Microbially-influenced corrosion capability of Yucca Mountain bacterial isolates. *Proceedings of the Seventh Annual International Conference on High-Level Radioactive Waste Management*. La Grange Park, IL: American Nuclear Society: 12–18.

Pourbaix, M. 1974. *Atlas of Electrochemical Equilibria in Aqueous Solutions*. Houston, TX: National Association of Corrosion Engineers: 307–321.

Raman, R.K.S., A.S. Khanna, R.K. Tiwari, and J.B. Gnanamoorthy. 1992. Influence of grain size on the oxidation resistance of 2 1/4Cr-1Mo steel. *Oxidation of Metals*. 37 (1/2): 1–12.

Scully, J.R., and H.P. Hack. 1984. Galvanic corrosion prediction using long- and short-term polarization curves. *CORROSION/84*. Paper No. 34. Houston, TX: National Association of Corrosion Engineers.

Stahl, D., and J.K. McCoy. 1995. Impact of thermal loading on waste package material performance. *Scientific Basis for Nuclear Waste Management XVIII Symposium Proceedings*. Pittsburgh, PA. Materials Research Society: 671–678.

Szklarska-Smialowska, Z. 1986. *Pitting Corrosion of Metals*. Houston, TX: National Association of Corrosion Engineers: 224–231.

TRW Environmental Safety Systems, Inc., 1994. *Initial Summary Report for Repository/Waste Package Advanced Conceptual Design*. CRWMS No. B00000000-01717-5705-00015. Rev. 00, Las Vegas, NV: TRW Environmental Safety Systems, Inc.

TRW Environmental Safety Systems, Inc. 1995a. *Total System Performance Assessment—1995: An Evaluation of the Potential Yucca Mountain Repository*. B00000000-01717-2200-00136. Las Vegas, NV: TRW Environmental Safety Systems, Inc.

28/51

TRW Environmental Safety Systems, Inc. 1995b. *Controlled Design Assumptions Document.* B00000000-01717-4600-00032 Rev. 02. Las Vegas, NV: B00000000-01717-2200-00136. Las Vegas, NV: TRW Environmental Safety Systems, Inc.

TRW Environmental Safety Systems, Inc. 1995c. *Strategy for Waste Containment and Isolation for the Yucca Mountain Site. Preliminary YMSCO Review Draft.* Las Vegas, NV: TRW Environmental Safety Systems, Inc.

TRW Environmental Safety Systems, Inc. 1996. *Mined Geologic Disposal System Advanced Conceptual Design Report. Vol. III of IV. Engineered Barrier Segment/Waste Package.* B00000000-01717-5705-00027. Rev. 00. Las Vegas, NV: TRW Environmental Safety Systems, Inc.

Wilson, M.L., J.H. Gauthier, R.W. Barnard, G.E. Barr, H.A. Dockery, E. Dunn, R.R. Eaton, D.C. Guerin, N. Lu, M.J. Martinez, R. Nilson, C.A. Rautman, T.H. Robey, B. Ross, E.E. Ryder, A.R. Schenker, S.A. Shannon, L.H. Skinner, W.G. Halsey, J.D. Gansemer, L.C. Lewis, A.D. Lamont, I.R. Triay, A. Meijer, and D.E. Morris. 1994. *Total-System Performance Assessment for Yucca Mountain—SNL Second Iteration (TSPA-1993).* Vols. 1 & 2. SAND93-2675. Albuquerque, NM: Sandia National Laboratories.

3 KEY TECHNICAL ISSUE: RADIONUCLIDE TRANSPORT

3.1 SCOPE OF REVIEW

The portions of TSPA-95 relevant to the KTI concerning processes that may affect radionuclide transport from the repository to the accessible environment are identified in table 3-1.

Table 3-1. Total System Performance Assessment 1995 scope of review for the Key Technical Issue: Radionuclide Transport

Section	Title
6.5	Radionuclide Transport Modeling
7.4.4	Fracture/Matrix Interaction in the Geosphere
7.4.6	Radionuclide Retardation
9.2.4	Fracture/Matrix Interaction in the Geosphere

3.2 AREA OF CONCERN: FRACTURE/MATRIX INTERACTIONS

3.2.1 Description of the Total System Performance Issue

The fraction of radionuclide transport in fractures in the unsaturated zone is shown in TSPA-95 to be an important variable affecting overall performance measures. If fracture flow dominates water flux, the water that would ultimately interact with waste forms and carry radionuclides through the unsaturated zone would flow in fractures. Waste species would then have to be transferred to the matrix from fractures in order to rely on the favorable characteristics of slow water flow and large surface areas available for sorption. For fracture flow radionuclide travel times are predicted to be short. If radionuclide transfer from fractures to the matrix is limited, this alternate conceptual model could lead to predictions of repository performance that differ substantially from models in which flux is primarily or exclusively in the matrix.

A variety of geochemical evidence summarized in this report suggests that transfer of chemical species from fracture water to matrix water is limited under natural conditions. The process of solute transport from water flowing in fractures into a porous rock matrix is referred to as matrix diffusion (Neretnieks, 1980). This process generally occurs by molecular diffusion as a result of concentration gradients; however, in unsaturated systems, mechanisms such as water imbibition can achieve comparable effects on transport. Once in the matrix, contaminants may be transported at relatively slow rates compared to those along fracture paths because of minimal flow velocities in the matrix (i.e., long radionuclide residence times). Migration of contaminants from the matrix into the fracture occurs when the concentration in the fracture water diminishes below that in the matrix water or when the matrix becomes fully saturated and excess water flows into the fractures. The significance of matrix-diffusion like effects arising from fracture/matrix interactions in unsaturated media has yet to be demonstrated by laboratory or field experiments. In addition, some DOE studies (Thoma et al., 1992) indicate that mineral coatings on fracture walls may limit water imbibition into the matrix.

3.2.2 Description of the Department of Energy Approach and/or Position

It is acknowledged in TSPA-95 that better models are needed to describe nonequilibrium fracture-matrix interactions. An approximate nonequilibrium flow regime was employed in one set of fracture flow initiation conditions in which fracture flow was permitted in an equivalent continuum model when matrix saturation was only 95 percent. Fracture flow for TSPA-95 models in general was a small fraction of total water flux. This variable was from 0 for the Calico Hills nonwelded vitric unit for all low infiltration models. However, for relatively high (2 mm/y) infiltration fluxes the fraction of flow in fractures for the Calico Hills nonweld zeolitic unit was varied from 0.259 to 0.726. Furthermore, fractures were assumed not generally to be connected across hydrostatigraphic units. Radionuclides transported by fracture flow were assumed to be redistributed between fracture and matrix water according to relative fracture and matrix fluxes across hydrostratigraphic boundaries. Consequently the models predicted a small radionuclide flux to occur entirely by fracture flow.

Matrix diffusion was not treated explicitly in TSPA-95 as a mechanism for slowing the migration of radionuclides through the unsaturated and saturated zones. Rather, TSPA-95 used a Markov process algorithm to account for flow interactions between fractures and matrix; this approach had the net effect of increasing average radionuclide residence times in the matrix in a manner comparable to that of very effective matrix diffusion. As shown in the NRC-CNWRA audit review (Baca and Brient, 1996) of TSPA-95, use of the Markov fracture/matrix transitioning model leads to large particle travel times in the unsaturated zone (figure 2-2, section 2.2.3, Baca and Brient, 1996). It is stated in TSPA-95 (page 9-23) that "In the extreme case of equilibrium matrix diffusion ..., the solutes in fractures would travel at the same velocity as solutes in the matrix, and the effect would be the same as having matrix-flow only." The assumption of equilibrium matrix diffusion appears to represent the least conservative case of fracture/matrix interactions with regard to repository performance. The conservative bound of matrix diffusion corresponds to all transport in fractures and no interactions with the matrix, which was not modeled in TSPA-95. (The closest case to this is where the Markov transition length is assumed to be 1/100h where h represents the path legth in the stratum). Sensitivity studies reported in TSPA-95 (section 9.2.4) show that only when the Markov transition path lengths are large (i.e., small Markov transition rates) does the model yield fast arrival times, as would occur due to fracture flow.

3.2.3 Detailed Review Approach

Although individual hydrological and geochemical data sets may have multiple plausible explanations, geochemical data [described from the vicinity of YM, from the natural analog site at Peña Blanca, Mexico, and from the Apache Leap Test Site (ALTS)] suggest that matrix diffusion type processes may have a limited effect and that intersecting fracture networks connect across hydrostratigraphic boundaries under hydrologic conditions relevant to the proposed repository site. These data are described specifically in the following sections.

3.2.3.1 Water Chemistry Comparative Analysis and Bomb Pulse Isotopes

Murphy and Pabalan (1994) summarized reported groundwater chemistry data from the saturated zone in the vicinity of YM, from the unsaturated zone at YM, from fractures with water flowing into tunnels above the water table at Rainier Mesa, and from interstitial pores in rocks from the unsaturated zone at Rainier Mesa (figure 3-1). Rainier Mesa is located approximately 30 km north of YM in a similar geologic setting but at a higher elevation with greater rainfall and groundwater recharge. Generally, these waters have similar chemistries, with some exceptions for the unsaturated zone matrix waters at YM.

Generally these waters are dilute; pH is generally between 7 and 8; Na^+ and HCO_3^- are predominant ions; and dissolved SiO_2 is significantly in excess of saturation with respect to quartz. Fracture water at Rainier Mesa has chemical characteristics that particularly correspond closely to characteristics of saturated zone groundwaters in the tuffaceous aquifer in the vicinity of YM. This similarity suggests that fracture waters at Rainier Mesa represent the type of recharge that supplies the saturated zone tuffaceous aquifer in the vicinity of YM.

In contrast, interstitial unsaturated zone waters from Rainier Mesa have higher Cl^- and SO_4^{2-} contents than fracture water at Rainier Mesa. These data may reflect partial evaporation of imbibed matrix water, with controls on cation concentrations, pH, and HCO_3^- by gas-water-rock interactions. Differences between fracture and matrix water chemistries may indicate that interactions between fracture and matrix water in Rainier Mesa are limited.

Unsaturated zone waters from YM exhibit numerous chemical differences from YM saturated zone water and from both fracture and unsaturated zone waters from Rainier Mesa. Except for Na^+ and possibly HCO_3^- (for which there are limited published data), all dissolved constituent concentrations analyzed in the unsaturated zone waters extracted from drill cores at YM are high relative to other waters in this set (figure 3-1). For example, Ca^{2+}, Mg^{2+}, and Cl^- are up to 10 times more concentrated in YM unsaturated zone pore waters than in the saturated zone tuffaceous aquifer. Dissolved SiO_2 levels are consistently 50 percent greater in the matrix. Evaporation of varying degrees and long residence times are the most plausible mechanisms for generating waters with these characteristics.

Preliminary data (Yang et al., 1996) indicate that perched zone water chemistry at YM differs from the chemistry of pore waters extracted from YM unsaturated core samples collected outside areas of perched water. Perched water chemistry at YM is similar to saturated zone groundwater. For example, perched water chloride concentrations are approximately one-tenth of the pore water chloride concentrations (Yang et al., 1996). Lack of similarity indicates that the source and sink of the perched water is flow through fractures. The observations that the chemical characteristics between the fracture and matrix are distinct support the argument that fracture/matrix interactions are probably limited. Perched water zones, being fed by interconnected fractures, may be exceptions where significant interaction between the fracture water and matrix water can occur.

Data for ^{14}C, ^{3}H (Yang, 1992), and ^{36}Cl (Fabryka-Martin et al., 1996) derived from nuclear weapons testing have been collected from samples collected at depth at YM. Numerous occurrences of ^{36}Cl have been detected in the Exploratory Studies Facility at the repository horizon. These data indicate that rapid and localized transport can occur along well-connected fracture pathways in the unsaturated zone at YM permitting minimal interactions between fractures and matrix. The occurrence of bomb pulse isotopes at depth also indicates that fast flow paths are connected between hydrostratigraphic units.

Collectively these geochemical data suggests that flow and transport in the unsaturated zone may be better represented by a conceptual (and mathematical) models considering fast pathways (Ho et al., 1995; Altman et al., 1996) and limited fracture/matrix interactions than the predominant matrix flow conceptualization implicit in the TSPA-95 models.

3.2.3.2 Saturated Zone Characterization

Geochemical data also provide indications of ineffective matrix diffusion in the saturated zone tuffaceous aquifer at YM. Murphy (1995) offered several lines of evidence indicating that water extracted

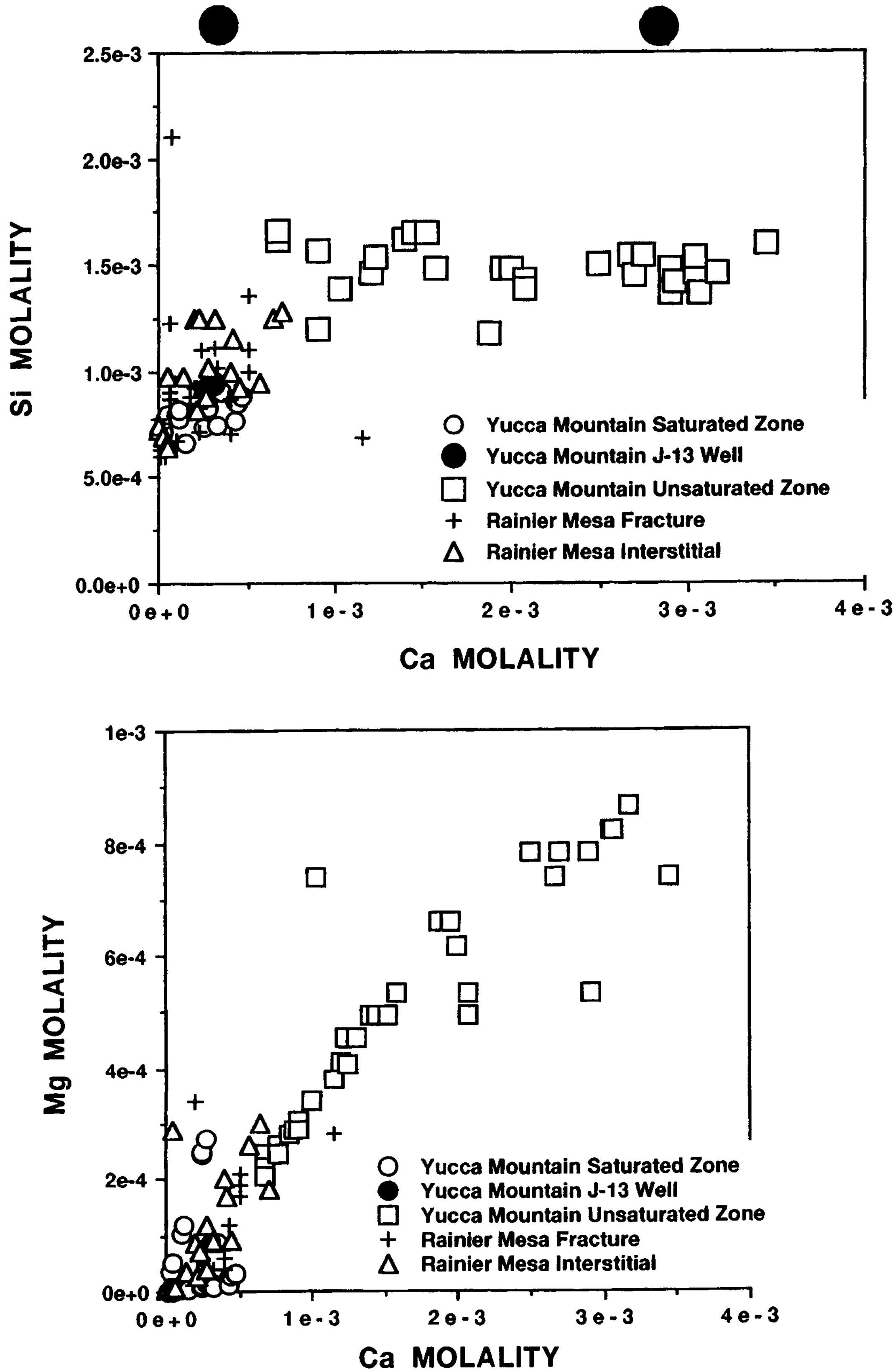

Figure 3-1. Water chemistry data from Yucca Mountain and vicinity summarized in Murphy and Pabalan (1994)

33/51

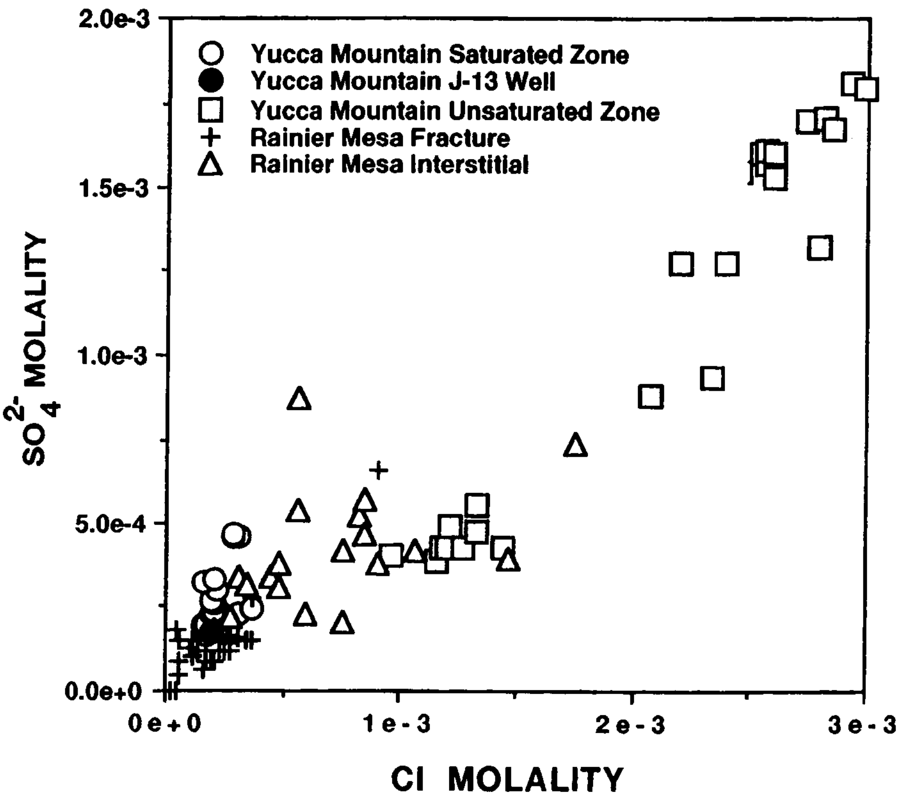

Figure 3-1. Water chemistry data from Yucca Mountain and vicinity summarized in Murphy and Pabalan (1994) (Cont'd)

from boreholes is not in chemical contact with parts of the rock matrix even over geologic time scales. Calcite is a common mineral in tuffaceous rocks from the vicinity of YM, although it is not generally abundant or ubiquitous. In tuffaceous rocks below the water table in the vicinity of YM, calcite occurs as milky veins and replacement cements. Saturated zone water however is chemically undersaturated with respect to calcite (figure 3-2) indicating isolation of that part of the rocks containing calcite from water flowing in the tuffaceous aquifer.

The carbon isotopic composition of calcite in tuffaceous rocks from greater than 300 m below the water table ($\delta^{13}C = -2$ to 5 °/oo) is generally compatible with precipitation from water that presently occurs in the deeper regional aquifer in Paleozoic carbonate rocks ($\delta^{13}C = -5.2$ to -2.3 °/oo). Carbonate aquifer water is isotopically different than water in the tuffaceous aquifer at YM ($\delta^{13}C = -11.4$ to -4.9 °/oo) (Whelan and Stuckless, 1992). These isotopic data also provide an indication of isolation of calcite from the groundwater flow system (Murphy, 1995). Indications that the calcite is old (e.g., 10 Ma; Bish and Aronson, 1993) argue for minimal effects of matrix diffusion in the saturated tuffaceous aquifer even over geologic time scales.

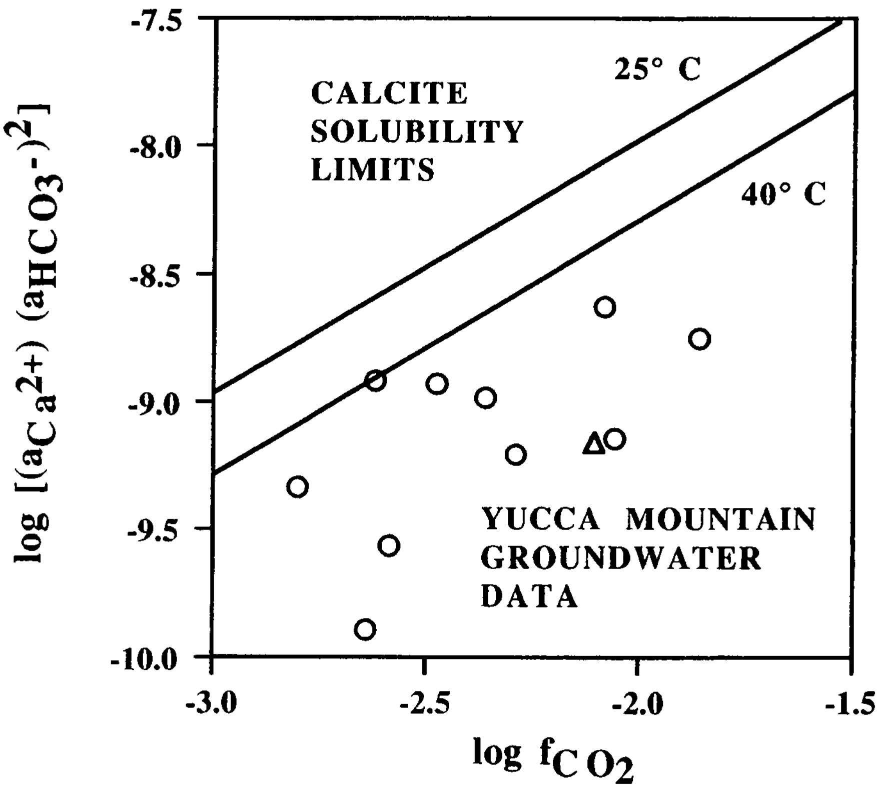

Figure 3-2. Logarithmic activity-fugacity diagram illustrating the solubility of calcite as a function of water chemistry and temperature (adapted from Murphy, 1995). Water with properties plotting above the solid lines is supersaturated with respect to calcite. Water with properties plotting below the lines is undersaturated with respect to calcite. Tuffaceous aquifer groundwaters from the vicinity of Yucca Mountain are plotted as open symbols.

Correspondence of calcite free zones with zones of relatively high permeability also supports the conclusion that flow in the tuffaceous aquifer is channelized and that much of the matrix is effectively chemically isolated (Murphy, 1995).

3.2.3.3 Nopal I Analog and Apache Leap Test Site

The Nopal I uranium deposit in the Peña Blanca District, Chihuahua, Mexico, has been studied as a natural analog of the proposed repository at YM. The site geology, hydrology, and climate bear remarkable similarities to YM. Uraninite (an analog of SF) was deposited in the rocks millions of years ago and now is nearly completely altered to secondary uranyl minerals. Formation of oxidized U minerals at the Nopal I deposit at Peña Blanca has been dated at three million years (Pickett et al., 1997). Alpha particle impact densities and alpha- and gamma-spectroscopy were used to determine U concentrations in the fractures and in the tuffaceous rock matrix adjacent to microfractures with infillings of U minerals. Some rocks are rich in U, but the boundary of U mineralization is sharp. In areas where the U deposit is in rocks adjacent to relatively unfractured tuff, elevated U concentrations in the tuff drop to background levels within distances of centimeters.

Figure 3-3 illustrates the sharply diminishing U concentrations over distances of less than 0.5 m from the edge of the zone of U mineralization at Nopal I (Pearcy et al., 1995). This almost negligible U transport into the rock matrix is, in part, indicative of the strong sorption properties of U. In contrast, certain major fractures at Nopal I contain anomalous U associated with Fe minerals at distances of tens of meters from the occurrence of uranium minerals (Pearcy et al., 1995; Pickett et al., 1997) (figure 3-4). It follows that U transport occurred primarily in fractures and that migration from fractures to the matrix is minimal.

Uranium in the deposit of visible U minerals is in secular isotopic equilibrium indicating that minimal U has been removed from this deposit in the past several hundred thousand years (Pearcy et al., 1995; Prikryl et al., 1997; Pickett et al., 1997). The U outside of the deposit is commonly out of secular equilibrium indicating some transport of U and deposition over the past few hundred thousand years. The U-series data indicate at least a two stage process of U deposition and remobilization in the last few hundred thousand years (Pickett et al., 1997). Mechanisms of U mobilization and precipitation of anomalous U in fractures are capable of transporting U over tens of meters along fracture pathways in hundreds of thousands of years.

Hydrologic and geochemical studies of flow and transport through unsaturated fractured tuff at the ALTS in Arizona have shown that the recharge and the flow system are dominated by discrete fracture pathways in a small subset of the numerous mappable fractures. Flow velocities in fractures during recharge events are greater than 60 m/day (Davidson et al., 1997). These results suggest that water residence times are too short to permit significant imbibition into the matrix. The data also suggest that fast transport paths can extend over distances of at least 120 m, perhaps crossing hydrostratigraphic boundaries.

3.3 DESCRIPTION OF THE LIKELY EFFECTS ON PERFORMANCE

Collectively, the geochemical data from YM and vicinity, the Nopal I deposit, and the ALTS indicate that water circulating in fracture flow pathways may be minimally affected by limited fracture/matrix interactions (i.e., matrix diffusion type effects). Comparable results from varied but relevant sites and hydrologic regimes indicate that the observation of limited fracture/matrix effects is robust as well as conservative. Radionuclide travel times in the proposed repository are unlikely to be as long as those consistent with TSPA-95 results and unlike the nonconservative case of matrix-flow-only transport that was tested in the TSPA-95 sensitivity studies. In developing its safety case for YM, the DOE should take credit for beneficial fracture/matrix interactions only if there is substantive laboratory or field evidence that demonstrates this process predominates.

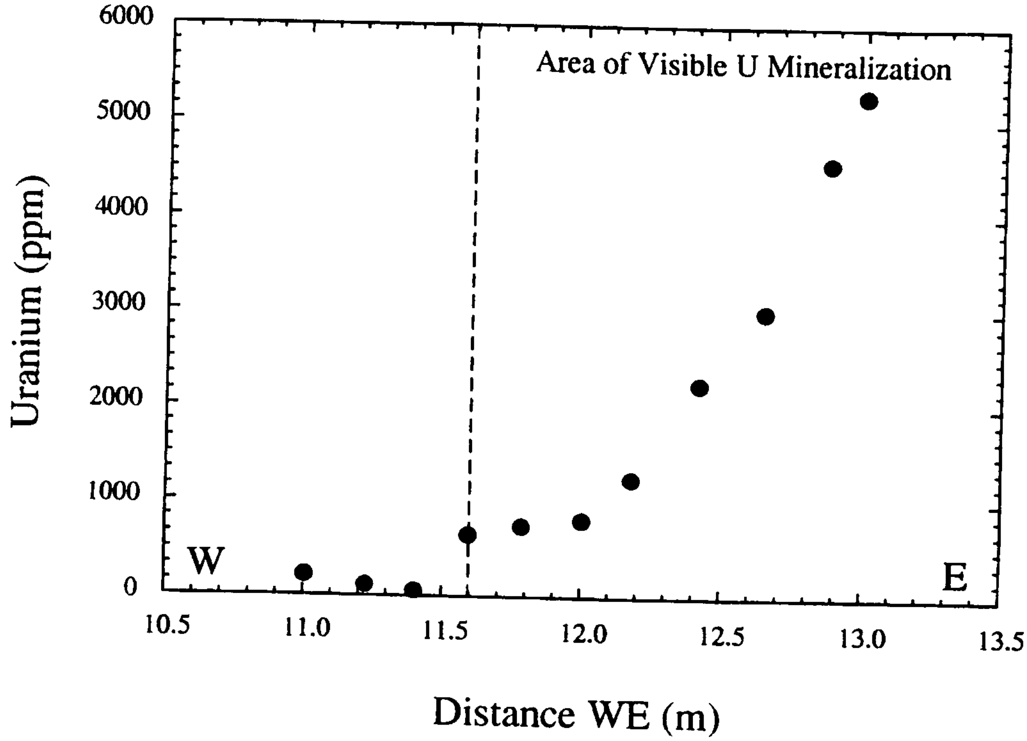

Figure 3-3. Uranium concentration in rock as a function of distance in a traverse at Nopal I (adapted from Pearcy et al., 1995). The dashed line represents the limit of visible uranium mineralization.

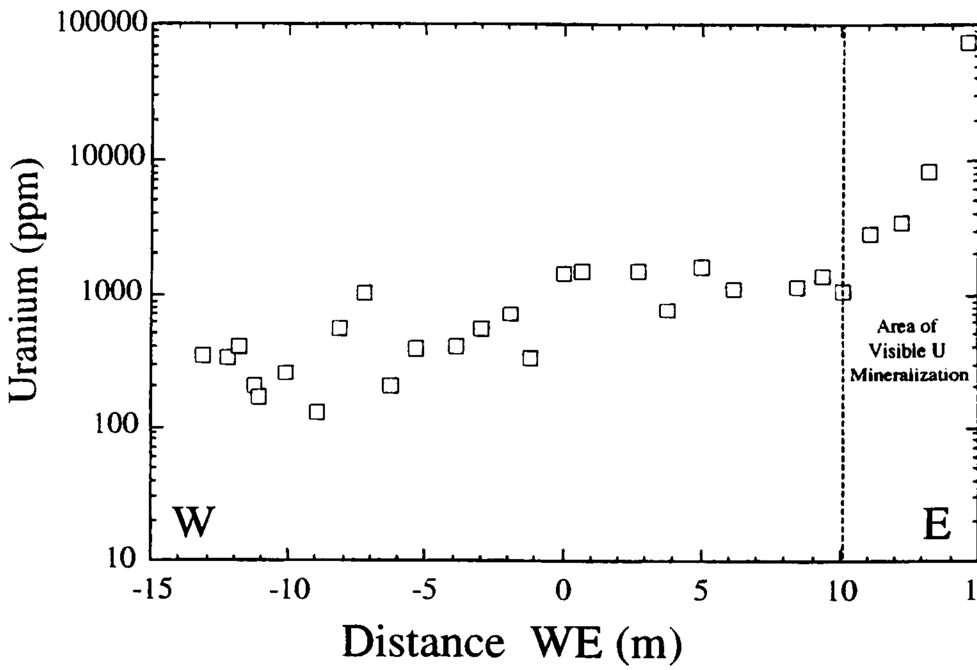

Figure 3-4. Uranium concentration in a fracture infilling material as a function of distance in a traverse along a major fracture at Nopal I (adapted from Pearcy et al., 1995). The dashed line represents the limit of visible uranium mineralization.

3.4 REFERENCES

Altman, S.J., B.W. Arnold, R.W. Barnard, G.E. Barr, C.K. Ho, S.A. McKenna, and R.R. Eaton. 1996. *Flow Calculations for Yucca Mountain Groundwater Travel Time (GWTT-95)*. SAND96-0819. Albuquerque, NM: Sandia National Laboratories.

Baca, R.G., and R.D. Brient. 1996. *Total System Performance Assessment 1995 Audit Review*. Letter Report. San Antonio, TX: Center for Nuclear Waste Regulatory Analyses.

Bish, D.L., and J.L. Aronson. 1993. Paleogeothermal and paleohydrologic conditions in silicic tuff from Yucca Mountain, Nevada. Clays and Clay Minerals 41: 148–161.

Davidson, G.R., R.L. Bassett, E.L. Hardin, and D.L. Thompson. 1997. Geochemical evidence of preferential flow of water through fractures in unsaturated tuff, Apache Leap, Arizona. *Applied Geochemistry*. Submitted for publication.

Fabryka-Martin, J.T., P.R. Dixon, S. Levy, B. Liu, H.J. Turin, and A.V. Wolfsberg. 1996. *Summary Report of Chlorine-36 Studies: Systematic Sampling for Chlorine-36 in the Exploratory Studies Facility*. LA-UR-96-1384. Los Alamos, NM: Los Alamos National Laboratory.

Ho, C.K., S.J. Altman, and B.W. Arnold. 1995. *Alternative Conceptual Models and Codes for Unsaturated Flow in Fractured Tuff: Preliminary Assessments for GWTT-95*. SAND95-1546. Albuquerque, NM: Sandia National Laboratories.

Murphy, W.M. 1995. Contributions of thermodynamic and mass transport modeling to evaluation of groundwater flow and groundwater travel time at Yucca Mountain, Nevada. *Scientific Basis for Nuclear Waste Management XVIII Symposium Proceedings*. T. Murakami, and R.C. Ewing, eds. Pittsburgh, PA: Materials Research Society: 353: 419–426.

Murphy, W.M., and R.T. Pabalan. 1994. *Geochemical Investigations Related to the Yucca Mountain Environment and Potential Nuclear Waste Repository*. NUREG/CR-6288. Washington, DC: Nuclear Regulatory Commission.

Neretnieks, I. 1980. Diffusion in the rock matrix: An important factor in radionuclide migration. *Journal of Geophysical Research*. 85(8): 1,749–1,758.

Pearcy, E.C., J.D. Prikryl, and B.W. Leslie. 1995. Uranium transport through fractured silicic tuff and relative retention in areas with distinct fracture characteristics. *Applied Geochemistry*. 10: 685–704.

Pickett, D.A., J.D. Prikryl, W.M. Murphy, and E.C. Pearcy. 1997. Uranium-series disequilibrium investigation of radionuclide mobility at the Nopal I uranium deposit, Peña Blanca District, Mexico. *Applied Geochemistry*. In preparation.

Prikryl, J.D., D.A. Pickett, W.M. Murphy, and E.C. Pearcy. 1997. Migration behavior of naturally-occurring radionuclides at the Nopal I uranium deposit, Chihuahua, Mexico. *Journal of Contaminant Hydrology*. In press.

38/51

Thoma, S.G., D.P. Gallegos, and D.M. Smith. 1992. Impact of fracture coatings on fracture/matrix flow interactions in unsaturated porous media. *Water Resources Research* 28(5): 1,357–1,367.

Whelan, J.F., and J.S. Stuckless. 1992. Paleohydrologic implications of the stable isotopic composition of secondary calcite within the Tertiary volcanic rocks of Yucca Mountain, Nevada. *Proceedings of the Third International Conference on High Level Radioactive Waste Management*. La Grange Park, IL: American Nuclear Society: 1,572–1,581.

Wilson, M.L., J.H. Gauthier, R.W. Bernard, G.E. Barr, H.A. Dockery, E. Dunn, R.R. Eaton, D.C. Guerin, N. Lu, M.J. Martinez, R. Nilson, C.A. Rautman, T.H. Robey, B. Ross, E.E. Ryder, A.R. Schenker, S.A. Shannon, L.H. Skinner, W.G. Halsey, J.D. Gansemer, L.C. Lewis, A.D. Lamont, I.R. Triay, A. Meijer, and D.E. Lewis. 1994. *Total-System Performance Assessment for Yucca Mountain—SNL Second Iteration (TSPA-1993)*. SAND93-2675. Vols. 1 & 2, Albuquerque, NM: Sandia National Laboratories.

Yang, I.C. 1992. Flow and transport through unsaturated rock -- data from two test holes, Yucca Mountain, Nevada. *Proceedings of the Third International Conference on High Level Radioactive Waste Management*. La Grange Park, IL: American Nuclear Society: 732–737.

Yang, C., G.W. Gordon, and P. Yu. 1996. *Interpretations of Chemical and Isotopic Data from Boreholes in the Unsaturated Zone at Yucca Mountain, Nevada*. WRIR 96-4058. Denver, CO: U.S. Geological Survey.

39/51

4 KEY TECHNICAL ISSUE: IGNEOUS ACTIVITY

4.1 SCOPE OF REVIEW

The portion of TSPA-95 concerning the prediction of the probability and consequences of igneous activity affecting the proposed repository in relation to the overall system performance is identified in table 4-1.

Table 4-1. Total System Performance Assessment 1995 scope of review for the Key Technical Issue: Igneous Activity

Section	Title
2.7.2	Volcanic Effects

4.2 AREA OF CONCERN: DISRUPTIVE SCENARIO—VOLCANISM

4.2.1 Description of the Total System Performance Issue

Basaltic volcanoes are capable of dispersing material for tens of kilometers away from the vent, depending on the ash particle size. Commonly, basaltic volcanoes also disrupt some volume of subsurface rock adjacent to the conduit and transport it with the erupting magma. Potential interactions between a basaltic magma and a HLW repository, however, are only generally constrained and are associated with large degrees of uncertainty. Specifically, the amount of HLW entrained into an erupting magma and the area over which this HLW is dispersed is an important aspect of total system performance risk assessment, but one that has no exact analog in nature.

4.2.2 Description of the U.S. Department of Energy Approach and/or Position

The technical basis for the DOE TSPA calculations regarding amount and dispersal of waste by volcanic activity is presented in Barr et al. (1993). The amount of waste released is constrained by the volume of subsurface rock contained in tephra deposits from a Yucca Mountain Region (YMR) volcano. This constraint has been evaluated by studies of Lathrop Wells and other basaltic cinder cones in the western U.S. thought to be analogous with YMR volcanoes. Studies of these volcanoes generally conclude that the volume of subsurface rock is less than 0.01 percent of the tephra deposits (Valentine and Groves, 1996). These studies have been used to support the assertion in TSPA-95 that volcanic processes have an insignificant effect on postclosure performance.

4.2.3 Detailed Review Approach

Current concerns with these modeling approaches are that the volume of waste erupted is likely underestimated by using subsurface rock abundances and that basaltic volcanoes of lesser dispersivity (i.e. power) than those of the YMR commonly disperse material coarser than 1 mm beyond 8 km from the vent.

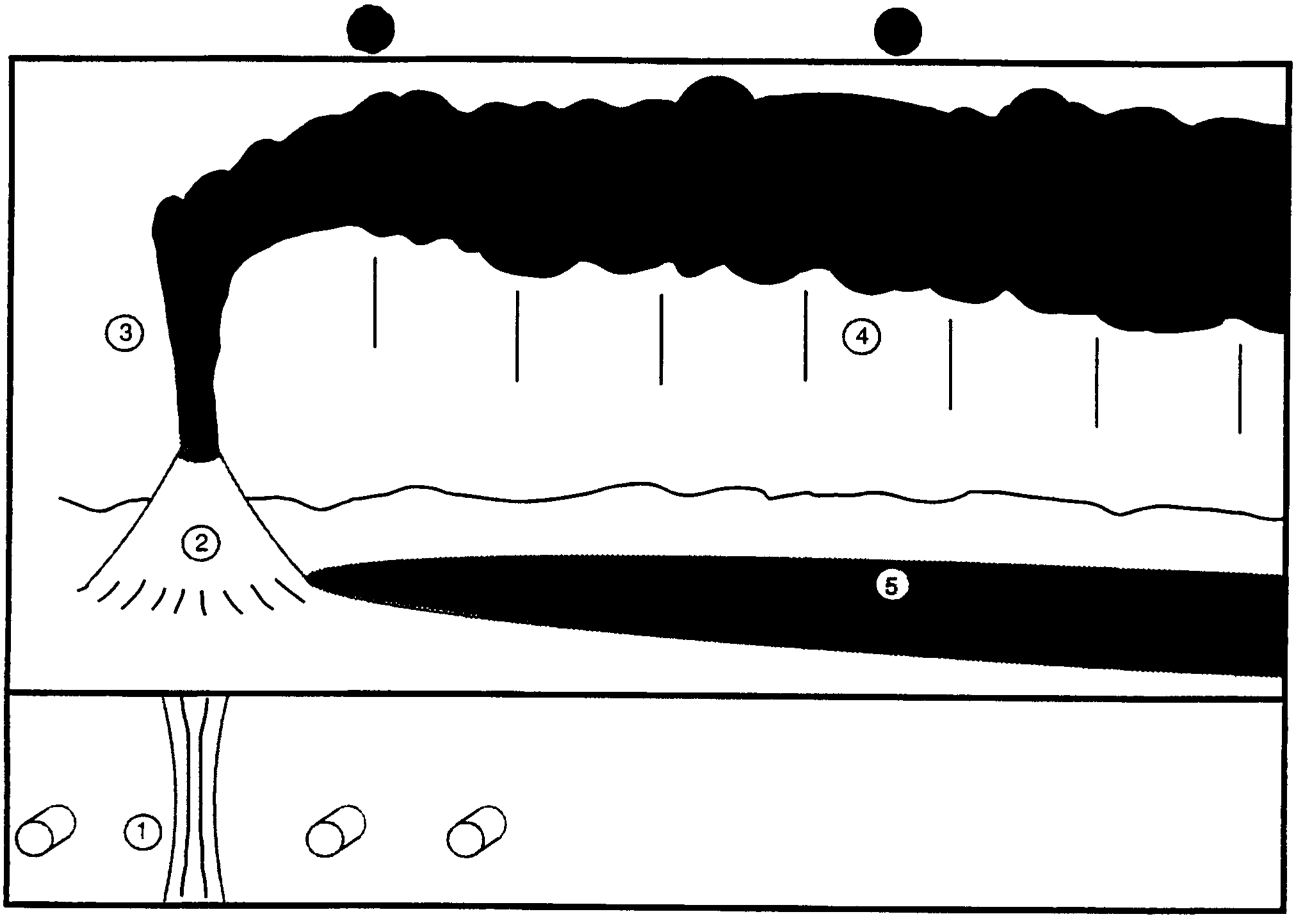

Figure 4-1. Diagram describing the volcanism exposure scenario

4.2.3.1 Probability Modeling

The probability of future igneous activity at the proposed YM repository site has been estimated using a range of nonhomogeneous Poisson models (e.g., Connor and Hill, 1995; Condit and Connor, 1996; Connor et al., 1996). These models account for observed spatio-temporal patterns in volcanism and result in probabilities of future igneous activity at the proposed 5.6 km^2 repository site of somewhat greater than 10^{-8} per year (Connor and Hill, 1995). Recent probability models in Connor et al. (1996) and Hill et al. (1996) directly incorporate site-specific geologic data. Faults with high dilation-tendency are potential conduits for future igneous events and the location of ascending magma also is likely controlled by large-scale crustal structures. Accounting for the locations of these geologic features in the YMR results in probabilities of future igneous activity at the proposed 5.6 km^2 repository site of 10^{-7} to 10^{-8} per year. This range is considered by the CNWRA staff to best represent the probability of future igneous activity at the proposed repository site and will form the basis for future issue resolution.

4.2.3.2 Consequence Modeling

Figure 4-1 shows the exposure scenario that was investigated in these analyses. The exposure scenario analyzed can be divided into four subprocesses:

- magma enters the repository and becomes contaminated with SF particles
- tephra forms from the magma and SF is incorporated into tephra (Jarzemba and LaPlante, 1996)
- eruption column and contaminant plume form and produce fallout at various distances downwind from the volcano (Suzuki, 1983; Jarzemba, 1996)
- conversion from radionuclide surficial concentration to peak annual total effective dose equivalent is performed for distances 20, 25, and 30 km directly south of the repository (LaPlante et al., 1995; Jarzemba and LaPlante, 1996)

A complete description of how these subprocesses were modeled is contained in the cited references.

Through preliminary investigations it was found that the parameters that most affect final dose estimates for a given amount of extruded fuel are the fuel particulate size distribution parameters (used to describe the assumed log-triangular distribution on fuel particulate size) and the incorporation ratio (Jarzemba and LaPlante, 1996). The parameters that describe the log-triangular fuel particulate size distribution are the lower limit of fuel particulate log-diameter, the mode of fuel particulate log-diameter distribution, and the upper limit of fuel particulate log-diameter where all diameters are expressed in centimeters. The incorporation ratio is described further in section 4.2.5.

4.2.4 Tephra Dispersal Modeling

Dispersed tephra deposits (i.e., ash), from all previous YMR basaltic volcanoes have been removed through erosion. Models used in performance assessments for tephra dispersion thus are constrained through comparison with appropriate data from analogous basaltic volcanoes. As discussed in Jarzemba (1996), the dispersion model of Suzuki (1983) is thought to best represent tephra dispersion. This mathematical model successfully reproduces, to within 50 percent, tephra deposit thicknesses measured during the 1995 eruption of Cerro Negro volcano in Nicaragua (Hill et al., 1996). This model represents an improvement over gaussian-plume dispersion models that model gravitational settling from a single release point (the stack height) and whose accuracy is at best within a factor of three for single point releases (e.g., Link et al., 1982; Cember, 1983). The Suzuki (1983) model is relatively sensitive to wind speed, whereas reasonable variations in other volcanological parameters such as tephra grain-size, density, and diffusion constants have minor effects on calculated deposit thicknesses (Hill et al., 1996).

A key parameter for the Suzuki (1983) model is the eruption column height, calculated from the tephra mass-flow rate (Jarzemba, 1996). Original implementations of the model in Jarzemba (1996) and Jarzemba and LaPlante (1996) used preliminary tephra mass-flow rates. These rates have been examined in detail for analog basaltic volcanoes and expanded to better represent the mass-flow rates deduced for YMR volcanoes. Measured column heights, eruption durations, and parameter values calculated from column height and eruption duration using equations in this report and Wilson et al. (1988) for these analog volcanoes are shown in table 4-2. Sources for observed data are Heimaey (Self et al., 1974), Paricutin (Luhr and Simkin, 1993), Tolbachik (Budnikov et al., 1983; Fedotov et al., 1984), Cerro Negro 1947 (McKnight, 1995), Cerro Negro 1968 (Viramonte and Di Scalia, 1970; Taylor and Stoiber, 1973), Cerro Negro 1971 (Viramonte et al., 1971; Rose et al., 1973), Cerro Negro 1992 and Cerro Negro. These eruptions range in total magmatic volume from 0.01 km^3 (Cerro Negro 1995) to 0.9 km^3 (Paricutin). After correcting for erosion, Quaternary YMR volcanoes range in total magmatic

Table 4-2. Observed column heights and eruption durations for 9 basaltic volcanic eruptions analogous to YMR volcanoes. Data sources and calculation methods in text.

Observed			Calculated				
	Column H (km)	Eruption Duration (s)	Height H (km)	Power Q (W)	Magma density t (kg/m^3)	Tephra mass flow v (m^3/s)	Magma temp T (°K)
Heimaey 1973	2	2.25×10^6	2.2	4.89×10^9	2600	2.3	1325
Paricutin 1943	4-6	7.26×10^6	4.0	5.73×10^{10}	2530	26.6	1375
Tolbachik Cone 1	6-10	1.21×10^6	4.8	1.14×10^{11}	2640	49.6	1400
Tolbachik Cone 2	2-3	3.28×10^6	3.5	3.18×10^{10}	2610	14.0	1400
Cerro Negro 1947	4-6.5	8.64×10^5	3.5	3.35×10^{10}	2600	15.9	1325
Cerro Negro 1968	1-1.5	3.63×10^6	1.9	2.62×10^9	2600	1.2	1325
Cerro Negro 1971	6	6.05×10^5	3.8	4.85×10^{10}	2600	23.0	1325
Cerro Negro 1992	6.5	6.39×10^4	6.4	3.64×10^{11}	2600	172.1	1325
Cerro Negro 1995	2	3.46×10^5	2.4	7.95×10^9	2600	3.8	1325

volume from 0.001 km^3 (Northern Cone) to 0.2 km^3 (Quaternary Crater Flat). Pliocene volcanoes have estimated volumes to at least 1 km^3 (e.g., Crowe et al., 1995). The historically active analog volcanoes in table 4-2 thus represent the same scale of basaltic volcanic features as found in the YMR.

Wilson et al. (1978) calculate eruption power or the steady rate of thermal energy release (Q) by

$$Q = t * v * s * (T_i - T_f) * F \qquad (4\text{-}1)$$

where t is the magmatic density in kg m^{-3}, v is the mass flow rate in $m^3\ s^{-1}$, s is the specific heat for basalt (estimated to be 1.1×10^3 J $kg^{-1}\ K^{-1}$; Wilson et al, 1978), T_i is the temperature of the erupting magma, T_f is the final temperature of the deposit (270 °K) and F is an efficiency factor (estimated to be 0.7; Wilson et al., 1978) for basaltic eruptions.

Following Wilson et al. (1978), the height of the eruption column (H) in m is then computed from eruption power (Q) in watts from

$$H = 8.2Q^{0.25} \qquad (4\text{-}2)$$

43/51

Eruption column heights calculated with Eqs. (4-2) and (4-3) are in reasonable agreement with measured column heights (table 4-2). The eruption power and duration data in table 4-2 are only weakly interrelated (figure 4-2). For the current analyses, power–duration parameters are sampled independently from log-uniform probability distributions between 2.6×10^9–3.64×10^{11} W power for and 6.39×10^4–7.26×10^6 s for duration.

4.2.5 In-depth Analyses for the Most Sensitive Parameters

The model that was used to track the movement of SF after a volcanic eruption does so by tracking the movement of contaminated ash that carries the SF (Jarzemba and LaPlante, 1996; Jarzemba 1996). Since convective columns and subsequent plumes are not capable of transporting large, dense particles to the distances analyzed in these calculations, the resulting doses are highly sensitive to the size distribution assumed for the SF particulate size. As mentioned earlier, SF is assumed to be accurately characterized by a log-triangular size distribution. Further, the upper and lower limits of this distribution are assumed to be plus and minus one order of magnitude from the mode. Three values for the mode of this distribution were analyzed to determine impact on dose: (i) 10 microns corresponding to the grain size of SF particles after irradiation in a reactor, (ii) 1 mm roughly corresponding to fuel particle sizes after irradiation in a reactor (Clark et al., 1985) and (iii) 1 cm corresponding to agglomerated fuel pellet sizes, possibly the result of repository forces over long times or coagulation from magma during the event. These fuel particle size distributions are referred to as low, med, and high in table 4-3. Three values for the incorporation ratio (ρ_c) were analyzed (0.3, 0.7, and 1.0) corresponding to a ratio of d^a_{min} to d^f_{max} of 2, 5, and 10, respectively. The incorporation ratio is defined as:

$$\rho_c = \log_{10} \frac{\left(d^a_{\min}\right)}{\left(d^f_{\max}\right)} \qquad (4\text{-}3)$$

where

d^a_{min} = the minimum ash particle size needed to incorporate fuel particles of size d^a_{max} or smaller

4.2.6 Results

The calculated impact of contaminated ash deposition (10 MTU of SF total contamination) on a hypothetical receptor group located due south of YM are shown in table 4-3, which is based on the methods described in the preceding section. These results were generated in part with the ASHPLUME code (Jarzemba et al., 1997). This code was developed by the NRC and the CNWRA for analyzing the consequences of an assumed volcanic disruption of the proposed repository in PAs of YM. The quantities listed in the table 4-3 are defined as follows

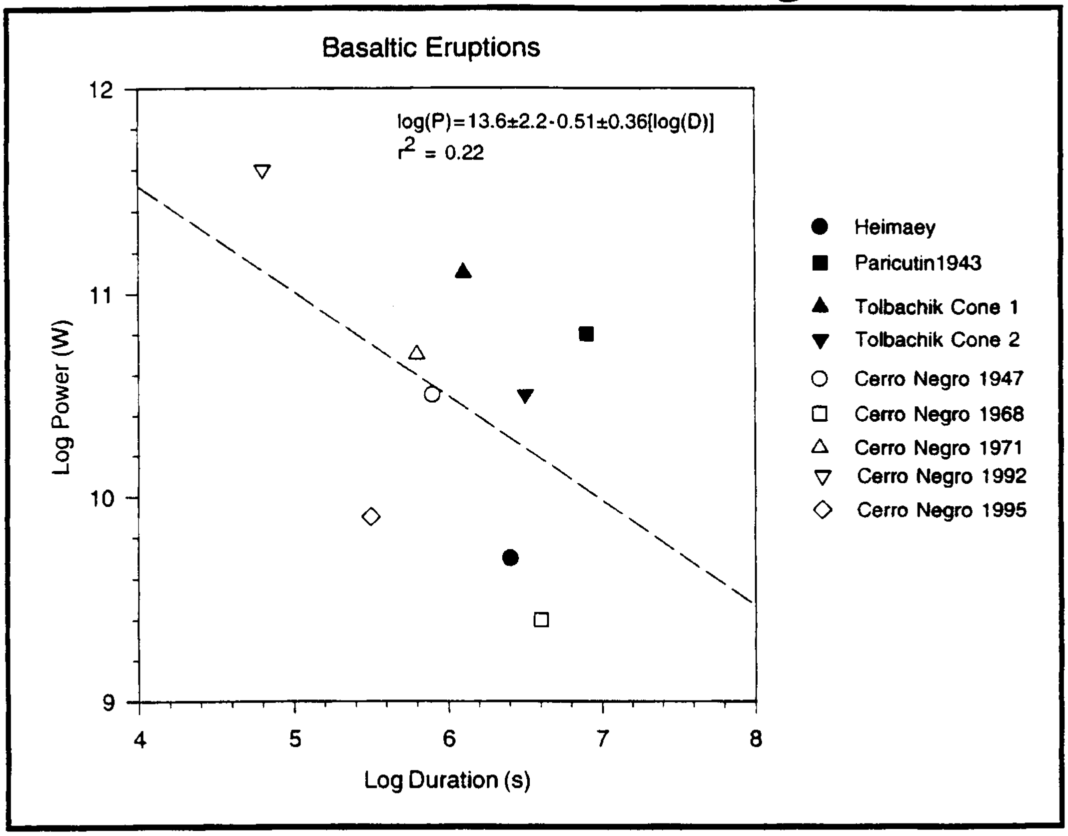

Figure 4-2. Power-duration plot for basaltic volcanoes listed in table 4-2. Note the low degree of correlation between these parameters, as shown by a linear regression correlation coefficient (r^2) of 0.22.

$$E(\dot{D}|V) \approx \bar{x} = p(u_{dir} = -90°) \cdot \frac{1}{N} \sum_{n=1}^{N} \dot{D}_n \qquad (4\text{-}4)$$

$$\sigma^2 \approx s^2 = p(u_{dir} = -90°) \cdot \frac{1}{N-1} \sum_{n=1}^{N} \left(\dot{D}_n - \bar{x}\right)^2$$

where

$E(\dot{D}|V)$ = The expected value of the parent distribution of the peak annual total effective dose equivalent in the Time Period of Interest (TPI) given that a volcano occurs

$\dot{D}_n$ = The n^{th} realization of the peak annual total effective dose equivalent in the TPI given that the wind is blowing south and a volcano occurs

$p(u_{dir} = -90°)$ = The probability that the wind is blowing south = 0.14045 (DOE, 1988)

N = The number of realizations (300 for each of the 9 cases shown)

σ^2 = The variance of the parent distribution of the peak annual total effective dose equivalent (TEDE) in the TPI given that a volcano occurs

Table 4-3. Expected doses and standard deviations for the nine cases given that an extrusive volcanic event occurs at Yucca Mountain (assumes one waste package disrupted)

Fuel Particulate Size Distribution	Incorporation Ratio	Expected dose at 20 km South $\bar{x}$, s (rem/yr)	Expected dose at 25 km South $\bar{x}$, s (rem/yr)	Expected dose at 30 km South $\bar{x}$, s (rem/yr)
low	low	4.66×10^{-2}, 3.33×10^{-1}	1.63×10^{-2}, 1.07×10^{-1}	6.49×10^{-3}, 4.40×10^{-2}
low	med	4.49×10^{-2}, 3.34×10^{-1}	1.52×10^{-2}, 1.04×10^{-1}	5.70×10^{-3}, 3.98×10^{-2}
low	high	4.22×10^{-2}, 3.28×10^{-1}	1.40×10^{-2}, 1.04×10^{-1}	4.46×10^{-3}, 3.52×10^{-2}
med	low	8.72×10^{-3}, 9.30×10^{-2}	1.52×10^{-3}, 1.82×10^{-2}	1.76×10^{-4}, 2.57×10^{-3}
med	med	2.13×10^{-3}, 2.45×10^{-2}	2.61×10^{-4}, 3.34×10^{-3}	2.08×10^{-5}, 3.21×10^{-4}
med	high	2.51×10^{-4}, 3.03×10^{-3}	8.48×10^{-6}, 1.27×10^{-4}	1.15×10^{-7}, 1.53×10^{-6}
high	low	1.62×10^{-6}, 2.18×10^{-5}	3.15×10^{-9}, 3.03×10^{-8}	1.04×10^{-11}, 1.79×10^{-10}
high	med	1.10×10^{-11}, 1.91×10^{-10}	1.32×10^{-18}, 3.03×10^{-17}	1.77×10^{-29}, 3.07×10^{-28}
high	high	1.64×10^{-21}, 2.84×10^{-20}	1.93×10^{-37}, 3.03×10^{-36}	0 ± 0

Of the nine cases considered in this analysis, the most conservative estimate of the expected value of the peak annual total effective dose equivalent, given that the volcanic event occurs, is 47 mrem per year. The experimental standard deviation of the 300 realizations for this case is 333 mrem per year. This most conservative case was found to be a low fuel particulate size distribution and a low incorporation ratio.

Based on the 300 realizations for each of the 9 cases (table 4-3), expected dose at 20 to 30 km from the repository site does not have a simple normal or log-normal distribution. In each case, the sample distributions are skewed by realizations that result in extremely low doses. For example, using

46/51

the highest dispersion case presented, in which fuel particle size distribution and the incorporation ratio are taken to be low and the critical group is 20 km from the site, 10 percent of the realizations result in doses less than 2.2×10^{-10} rem/yr, 50 percent of the realizations result in doses less than 1.6×10^{-3} rem/yr, and 90 percent of the realizations result in doses less than 1.24 10^{-1} rem/yr. A CCDF for this case is precented in figure 4-3. This and similar distributions for other scenarios give rise to comparatively large variances reported for expected dose.

4.2.7 Overall Risk

Calculations in table 4-3 assume one WP was dispersed by a volcanic eruption. Recent studies by Hill (1996) conclude that subsurface conduits for YMR-type basaltic volcanoes can widen to 49 ± 7 m in diameter during later stages of eruption. Some Quaternary YMR volcanoes also show evidence for this scale of subsurface disruption (Hill, 1996). A repository loading of 83 MTU per acre (U.S. Department of Energy, 1996) represents an average of 2.1×10^{-2} MTU m^{-2}. If the volcanic conduit widened to a circle 50 m in diameter, it could potentially disrupt an area of 1964 m^2. This area represents the potential disruption of 41 MTU. Assuming the WP contains 10 MTU (U.S. Department of Energy, 1996), 4 WPs thus could be disrupted by conduit widening using average thermal loads. Waste package design lengths are generally 5 m (U.S. Department of Energy, 1996). Assuming minimal spacing between WPs, a 50 m diameter conduit widening event could disrupt at the most 9 to 10 waste packages. Expected doses and standard deviations in table 4-3 can be scaled by the number of WPs potentially dispersed by a basaltic volcanic eruption.

Thus, using the finest particle-size and lowest fuel/ash incorporation ratio distributions, expected dose for a group located 20 km of the site is 184 mrem/yr for a volcanic eruption intersecting a repository with an average thermal load (i.e., disrupting 40 MTU of fuel). For medium to large particle-size distributions, calculated dose resulting from exhumation and dispersal of 4 to 10 canisters (i.e., 40 to 100 MTU waste) by volcanism is comparatively low, with expected doses of less than 90 mrem/yr and typically less than 1 mrem/yr. These comparatively low doses occur because most of the waste is deposited in the ash blanket less than 20 km from the site. Processes such as remobilization of contaminated ash by wind and water also are not considered in current analyses.

Proper calculation of the dose risk requires that the probability of the event be multiplied by the consequences of the event (dose rate). The probability density of future igneous events at the proposed 5.6 km^2 repository site is currently thought to be between 10^{-7} and 10^{-8}/yr, thus is between 10^{-3} and 10^{-4}. Thus, a conservative estimate of risk the probability of a volcanic disruption in 10,000 yr is presented in this report is 0.5 mrem/yr for extrusive basaltic volcanic activity (i.e., probability = 10^{-3}, low particle size and incorporation ratio, 20 km critical group). This estimate of risk is strongly dependent on assumptions made about volcanic events, impact on repository performance, and dose pathways.

4.3 DESCRIPTION OF LIKELY EFFECTS ON PERFORMANCE

Based on review of pertinent DOE TSPA literature (i.e., Link et al., 1982; Barr et al., 1993; Wilson et al., 1994) and consideration of basaltic volcanism, it is recommended that five topics be considered (i) behavior of the WP during interaction with ascending basaltic magma, (ii) radioactive waste grain-size distributions *in situ* and during magmatic transport, (iii) subsurface area of disruption by basaltic volcanoes, (iv) dispersal capabilities of YMR basaltic volcanoes, and (v) modification of igneous processes by the disturbed geologic setting of the repository. At present, few data are available to evaluate

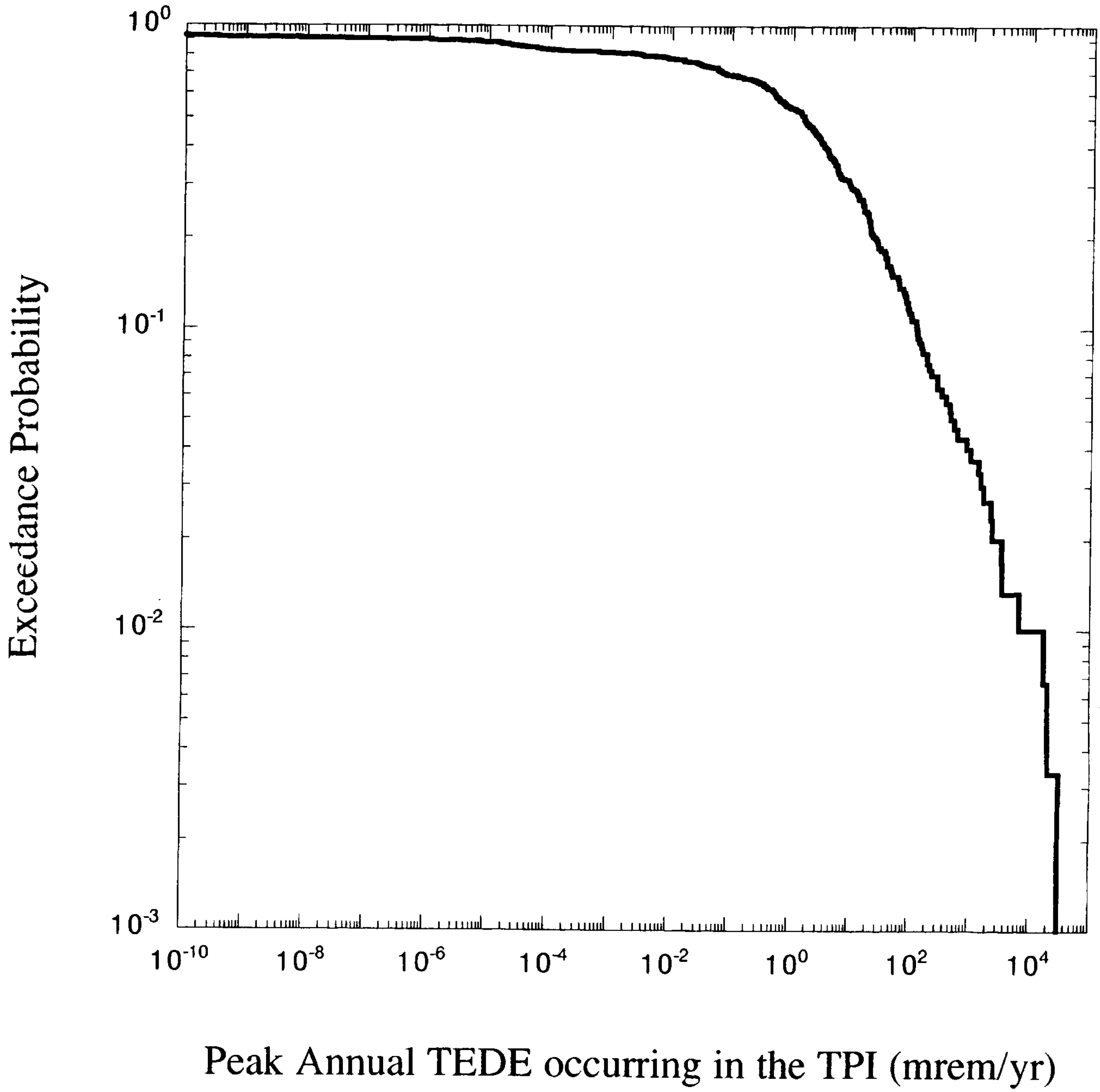

Figure 4-3. A plot of the complimentary cummulative distribution function of peak dose for the low incorporation ratio, low fuel particulate size case

48/51

effects of basaltic magma on WP integrity because basaltic magmas result in thermal, mechanical, and chemical loads beyond standard design criteria. Simple thermal considerations, however, show that waste canisters will likely fail under typical basaltic eruption conditions.

Current calculations follow the approach in the DOE TSPA, in which canisters in contact with basaltic magma are assumed to fail and make waste available for transport. Initial bounds on grain-size distributions of HLW are presented in this report and model sensitivities to this parameter are examined. The subsurface area of disruption controls the number of WPs that can be transported by the ascending magma. Recent work concludes that some recent YMR volcanoes had the capabilities to disrupt 50 m diameter areas at repository depths (Hill, 1996). The dispersal capabilities of YMR volcanoes have been discussed in Hill and Connor (1995), Hill et al. (1995) and Hill et al. (1996), which support the conclusion that these basaltic volcanoes can transport material tens of kilometers from the vent. The modification of igneous processes by the repository setting is part of planned investigations. Initial results of simple magma fragmentation models (i.e., subsurface disruption capability) are presented in Hill and Connor (1995).

Future TSPAs conducted by the DOE would be more defensible if volcanism was evaluated as a means of direct release and dispersal of radioactivity from the proposed YM repository in a manner similar to that described previously. These TSPAs should evaluate the release of HLW by incorporation into the erupting magma for intrusive and extrusive volcanic events with subsequent air dispersion and deposition of ash and radioactivity (for extrusive events) in the surrounding area.

4.4 REFERENCES

Barr, G.E., E. Dunn, H. Dockery, R. Barnard, G. Valentine, and B. Crowe. 1993. *Scenarios Constructed for Basaltic Igneous Activity at Yucca Mountain and Vicinity*. SAND 91-1653. Albuquerque, NM: Sandia National Laboratories.

Budnikov, V.A., Ye.K. Markhinin, and A.A. Ovsyannikov. 1983. The quantity, distribution and petrochemical features of pyroclastics of the great Tolbachik fissure eruption. S.A. Fedotov and Ye.K. Markhinin, eds. *The Great Tolbachik Fissure Eruption*. New York, NY: Cambridge University Press: 41–56.

Cember, H. 1983. *Introduction to Health Physics*. Second Edition. Elmsford, NY: Pergamon Press, Inc.

Clark, P.A.E., et al. 1985. *Post Irradiation Examination of Two High Burnup Fuel Rods Irradiated in the Halden BWR*. AEREG 3207. AERE Harwell Report.

Condit, C.D., and C.B. Connor. 1996. Recurrence rates of volcanism in basaltic volcanic fields: An example from the Springerville volcanic field, Arizona. *Geological Society of America Bulletin* 108: 1,225–1,241.

Connor, C.B., and B.E. Hill. 1995. Three nonhomogeneous Poisson models for the probability of basaltic volcanism: Application to the Yucca Mountain region, Nevada, U.S.A. *Journal of Geophysical Research* 100(B6): 10,107–10,125.

Connor, C.B., L. Powell, W. Strauch, M. Navarro, O. Urbina, and W.I. Rose. 1993. The 1992 eruption of Cerro Negro, Nicaragua: An example of Plinian–style activity at a small basaltic cinder cone. *EOS, Transactions, American Geophysical Union* 74–(43): 640.

Connor, C.B., J. Stamatakos, D.A. Ferrill, and B.E. Hill. 1996. Integrating structural models into probabilistic volcanic hazards analyses: An example from Yucca Mountain, Nevada. *Geological Society of America Abstracts with Programs* 28(7): A-192.

Crowe, B.M., F.V. Perry, J. Geissman, L. McFadden, S. Wells, M. Murrell, J. Poths, G.A. Valentine, L. Bowker, and K. Finnegan. 1995. *Status of Volcanic Hazard Studies for the Yucca Mountain Site Characterization Project.* LA–12908–MS. Los Alamos, NM: Los Alamos National Laboratory.

Fedotov, S.A., A.M. Chirkov, and A.A. Razina. 1984. Northern Breakout. S.A. Fedotov, ed. *Large Tolbachik Fissure Eruption, Kamchatka 1975–1976.* Moscow, Russia: Science: 11–74.

Hill, B.E. 1996. Constraints on the Potential Subsurface Area of Disruption Associated with Yucca Mountain Region Basaltic Volcanoes. San Antonio, TX: Center for Nuclear Waste Regulatory Analyses.

Hill, B.E., and C.B. Connor. 1995. Field Volcanism. *NRC High-Level Radioactive Waste Research at CNWRA, July-December 1994.* B.Sagar, ed. CNWRA 94-02S. San Antonio, TX: Center for Nuclear Waste Regulatory Analyses: 141–154.

Hill, B.E., F.M. Conway, C.B. Connor, and P. LaFemina. 1995. Field Volcanism. *NRC High-Level Radioactive Waste Research at CNWRA, January-June 1995.* CNWRA 95-01S. San Antonio, TX: Center for Nuclear Waste Regulatory Analyses: 7-1–7-22.

Hill, B.E., C.B. Connor and J.S. Trapp. 1996. Igneous Activity. *NRC High-Level Radioactive Waste Program Annual Progress Report, FY 1996.* NUREG/CR-6513, NO. 1. Washington, DC: NRC and CNWRA 97-01A. San Antonio, TX: Center for Nuclear Waste Regulatory Analyses. In press.

Jarzemba, M.S. 1996. Stochastic radionuclide distributions after a basaltic eruption for performance assessments of Yucca Mountain. *Nuclear Technology.* In press.

Jarzemba, M.S., and P.A. LaPlante. 1996. *Preliminary Calculations of Expected Dose from Extrusive Volcanic Events at Yucca Mountain.* San Antonio, TX: Center for Nuclear Waste Regulatory Analyses.

Jarzemba, M.S., P. LaPlante, and K.J. Poor. 1997. *Ashplume Code Version 1.0 Model Description and User's Guide.* CNWRA 97-004. San Antonio, TX: Center for Nuclear Waste Regulatory Analyses.

50/51

LaPlante, P.A., S.J. Maheras, and M.S. Jarzemba. 1995. *Initial Analyses of Selected Site-specific Dose Assessment Parameters and Exposure Pathways Applicable to a Groundwater Release Scenario at Yucca Mountain.* CNWRA 95-018. San Antonio, TX: Center for Nuclear Waste Regulatory Analyses.

Link, R.L., S.E. Logan, H.S. Ng, F.A. Rokenbach, and K.-J. Hong. 1982. *Parametric Studies of Radiological Consequences of Basaltic Volcanism.* SAND 81-2375. Albuquerque, NM: Sandia National Laboratories.

Luhr, J.F. and T. Simkin. 1993. *Paricutin—The Volcano Born in a Mexican Cornfield.* Phoenix, AZ: Geoscience Press, Inc.

McKnight, S.B. 1995. *Geology and Petrology of Cerro Negro Volcano, Nicaragua.* M.S. Thesis. Tempe, AZ: Arizona State University.

Rose, W.I., Jr., S. Bonis, R.E. Stoiber, M. Keller, and T. Bickford. 1973. Studies of volcanic ash from two recent Central American eruptions. *Bulletin Volcanologique* 37: 338–364.

Self, S., R.S.J. Sparks, B. Booth, and G.P.L. Walker. 1974. The 1973 Heimaey strombolian scoria deposit, Iceland. *Geological Magazine* 111: 539–548.

Suzuki, T. 1983. *A Theoretical Model for the Dispersion of Tephra.* D. Shimozuru and I. Yokiyama, eds. Arc Volcanism: Physics and Tectonics. Tokyo, Japan: Terra Scientific Publishing Company: 95–113.

Taylor, P.S., and R.E. Stoiber. 1973. Soluble material on ash from active Central America volcanoes. *Geological Society of America Bulletin* 84: 1,031–1,042.

TRW Environmental Safety Systems, Inc. 1996. *Mined Geologic Disposal System Advanced Conceptual Design Report. Vol. III of IV. Engineered Barrier Segment/Waste Package.* B00000000-01717-5705-00027. Rev. 00. Las Vegas, NV: TRW Environmental Safety Systems, Inc.

U.S. Department of Energy. 1988. *Site Characterization Plan.* DOE/RW-0199. Washington, DC: U.S. Department of Energy.

Valentine, G.A., and K.R. Groves. 1996. Entrainment of country rock during basaltic eruptions of the Lucero Volcanic Field, New Mexico. *Journal of Geology* 104: 71–90.

Viramonte, J.G., and L. Di Scalia. 1970. Summary of the 1968 eruption of Cerro Negro, Nicaragua. *Bulletin Volcanologique* 34(1): 347–351.

Viramonte, J.G., E. Ubeda, and M. Martinez. 1971. The 1971 eruption of Cerro Negro volcano, Nicaragua. *Smithsonian Institution Center for Short-Lived Phenomena Report 15 April 1971.* Washington, DC: Smithsonian Institution.

Wilson, L., R.S.J. Sparks, T.C. Huang, and N. D. Watkins. 1978. The control of volcanic column heights by eruption energetics and dynamics. *Journal of Geophysical Research* 83(B4): 1,829–1,836.

Wilson, M.L., J.H. Gauthier, R.W. Barnard, G.E. Barr, H.A. Dockery, E. Dunn, R.R. Eaton, D.C. Guerin, N. Lu, M.J. Martinez, R. Nilson, C.A. Rautman, T.H. Robey, B. Ross, E.E. Ryder, A. R. Schenker, S.A. Shannon, L.H. Skinner, W.G. Halsey, J.D. Gansemer, L.C. Lewis, A.D. Lamont, I.R. Triay, A. Meijer, and D.E. Morris. 1994. *Total-System Performance Assessment for Yucca Mountain—SNL Second Iteration (TSPA-1993)*. Vols. 1 & 2. SAND93-2675. Albuquerque, NM: Sandia National Laboratories.